BI-TP 2008/40
arXiv:0812.2105

Heavy quark medium polarization at next-to-leading order

Y. Burnier, M. Laine, M. Vepsäläinen

Faculty of Physics, University of Bielefeld, D-33501 Bielefeld, Germany

Abstract

We compute the imaginary part of the heavy quark contribution to the photon polarization tensor, i.e. the quarkonium spectral function in the vector channel, at next-to-leading order in thermal QCD. Matching our result, which is valid sufficiently far away from the two-quark threshold, with a previously determined resummed expression, which is valid close to the threshold, we obtain a phenomenological estimate for the spectral function valid for all non-zero energies. In particular, the new expression allows to fix the overall normalization of the previous resummed one. Our result may be helpful for lattice reconstructions of the spectral function (near the continuum limit), which necessitate its high energy behaviour as input, and can in principle also be compared with the dilepton production rate measured in heavy ion collision experiments. In an appendix analogous results are given for the scalar channel.

January 2009

1. Introduction

Heavy fermion vacuum polarization, i.e. the contribution of a massive fermion species to the (imaginary part of the) photon polarization tensor, or to the spectral function of the electromagnetic current, is one of the classic observables of relativistic quantum field theory: the result has been known up to 2-loop, or next-to-leading, or $\mathcal{O}(\alpha_s)$ level already since the 1950s [1].[1] Nevertheless, significant new insights were still obtained in the 1970s [2] and even in the 1990s [3]. By now a lot of information is also available concerning corrections of $\mathcal{O}(\alpha_s^2)$ and $\mathcal{O}(\alpha_s^3)$ (for recent work and references, see ref. [4]). The physics motivation for the continued interest is related, for example, to determining the heavy quark production cross section, $\sigma(e^-e^+ \longrightarrow c\,\bar{c})$, often expressed through the R-ratio, as well as to computing the heavy quarkonium decay width.

In the present paper, we consider essentially the same observable as in the classic works, but in a situation where the heavy quarks live at a finite temperature, T, rather than in the vacuum. We refer to this observable as the "heavy quark medium polarization". Again the result has direct physical significance, in that it determines the heavy quark contribution to the production rate of lepton–antilepton pairs from the thermal plasma [5] (cf. eq. (2.2) below). There has been considerable phenomenological interest particularly in what a finite temperature does to the resonance peaks in the spectral function, given that this might yield a gauge for the formation of a deconfined partonic medium [6]. Some recent work on the resonance region within the weak-coupling expansion, taking steps towards a systematic use of effective field theory techniques to resum appropriate classes of higher loop orders, can be found in refs. [7]–[11] (see ref. [12] for a review and ref. [13] for an alternative approach with similar results), and recent reviews on some of the phenomenological approaches on the market can be found in refs. [14, 15] (possible pitfalls of *ad hoc* potential models at finite temperatures have been reviewed in ref. [16], and underlined from a different perspective in ref. [13]). Analogous spectral functions can also be determined for theories with gravity duals [17].

Unfortunately, it appears that ultimately weak-coupling (and related) techniques will be insufficient for determining quantitatively the shape of the spectral function around the resonance region. The reason is that field theory at finite temperatures suffers from infrared problems, implying that the weak-coupling series goes in powers of $(\alpha_s/\pi)^{1/2}$ rather than α_s/π, often with large (sometimes non-perturbative [18]) coefficients; see, e.g., ref. [19] and references therein. Therefore, particularly for the case of charmonium where even at zero temperature weak-coupling computations can hardly be trusted, it appears that non-perturbative techniques are a must. Even though the situation should be somewhat better under control

[1] The older computations were formulated within QED, but at this order the results carry over directly to QCD, whose notation we adopt.

for bottomonium, a crosscheck by lattice methods would still be more than welcome.

On the point of lattice techniques, however, we are faced with a rather fundamental problem. Lattice techniques are applicable in Euclidean spacetime, while the spectral function is an inherently Minkowskian object. In principle the spectral function *can* be obtained through a certain analytic continuation of the Euclidean correlator; however, as a mathematical operation, at finite temperatures such an analytic continuation is unique only if the asymptotic behaviour for large Minkowskian arguments is known (see, e.g., ref. [20]). In a practical setting, many further problems arise because lattice data is not analytic in nature; yet the need to input outside information ("priors") to the analysis certainly remains a central issue (see refs. [21] for recent lattice results, and ref. [22] for an overview).

It is at this point that weak-coupling techniques may again become helpful. The goal would now be not so much to determine the spectral function around the resonance region, but to determine it at very high energies, which information should be relatively reliable, thanks to asymptotic freedom. Indeed, the *free* thermal spectral function has been studied in great detail previously, even at a finite lattice spacing [23]. Nevertheless, loop corrections are expected to remain substantial even up to energy scales of several tens of GeV, so it is important to account for them, and this is the basic goal of the present work. As a more refined goal, we wish to demonstrate that thermal corrections are small far away from the threshold; thereby knowledge of the asymptotic behaviour could be taken to higher orders, by employing well-known numerically-implemented results from zero temperature [24] (this assumes, of course, that a continuum extrapolation can be carried out on the lattice).

Apart from this lattice-related goal, we also wish to pursue the complementary goal of treating the bottomonium spectral function without any exposure to the often hard-to-control systematic uncertainties of lattice simulations. This can be achieved by constructing an interpolation between the asymptotic result determined in the present paper, and the near-threshold behaviour estimated within a resummed framework in ref. [8].

The plan of the paper is the following. In sec. 2 we define the observable to be computed. The general strategy of the computation is discussed in sec. 3, and the main results are summarized in sec. 4. A phenomenological reconstruction of the spectral function in the whole energy range is carried out in sec. 5, while sec. 6 lists our conclusions. In appendix A, we display in some detail the intermediate steps entering the determination of one of the "master" sum-integrals appearing in the computation; in appendix B, we list the final results for all the master sum-integrals; and in appendix C we provide results for the spectral function in the scalar channel, discussing briefly also the ambiguities that hamper this case.

2. Basic definitions

The heavy quark contribution to the spectral function of the electromagnetic current can be defined as

$$\rho_V(\omega) \equiv \int_{-\infty}^{\infty} \mathrm{d}t\, e^{i\omega t} \int \mathrm{d}^{3-2\epsilon}\mathbf{x} \left\langle \frac{1}{2}\left[\hat{\mathcal{J}}^\mu(t,\mathbf{x}), \hat{\mathcal{J}}_\mu(0,\mathbf{0})\right] \right\rangle \,, \tag{2.1}$$

where $\hat{\mathcal{J}}^\mu \equiv \hat{\bar{\psi}}\gamma^\mu\hat{\psi}$; $\hat{\psi}$ is the heavy quark field operator in the Heisenberg picture; $\langle\ldots\rangle \equiv \mathcal{Z}^{-1}\mathrm{Tr}\,[(...)e^{-\beta\hat{H}}]$ is the thermal expectation value; $\beta \equiv 1/T$ is the inverse temperature; and we assume the metric convention $(+---)$. This spectral function determines the production rate of muon–antimuon pairs from the system [5],

$$\frac{\mathrm{d}N_{\mu^-\mu^+}}{\mathrm{d}^4x\,\mathrm{d}^4q} = \frac{-2e^4Z^2}{3(2\pi)^5q^2}\left(1+\frac{2m_\mu^2}{q^2}\right)\left(1-\frac{4m_\mu^2}{q^2}\right)^{\frac{1}{2}} n_{\mathrm{B}}(\omega)\rho_V(\omega)\,, \tag{2.2}$$

where Z is the heavy quark electric charge in units of e, and n_{B} is the Bose-Einstein distribution function. In defining eq. (2.1) and the argument of ρ_V in eq. (2.2), we have assumed that the muon–antimuon pair is at rest with respect to the thermal medium, i.e. $q \equiv (\omega,\mathbf{0})$.[2] The pole mass of the heavy quark (charm, bottom) is denoted by M.

The parametric temperature range we concentrate on in this paper is the one where the "quarkonium" resonance peak disappears from the spectral function ρ_V [8]:

$$g^2M < T < gM\,. \tag{2.3}$$

This implies that in any case $T \ll M$, so that exponentially small corrections, $\sim \exp(-\beta M)$, can well be omitted. The thermal effects come thereby exclusively from the gluonic sector, where no exponential suppression takes place.

In order to compute the spectral function ρ_V of eq. (2.1), we start by determining the corresponding Euclidean correlator,

$$C_E(\omega_n) \equiv \int_0^\beta \mathrm{d}\tau\, e^{i\omega_n\tau} \int \mathrm{d}^{3-2\epsilon}\mathbf{x} \left\langle \hat{\mathcal{J}}^\mu(\tau,\mathbf{x})\hat{\mathcal{J}}_\mu(0,\mathbf{0})\right\rangle \,, \tag{2.4}$$

for which a regular path-integral expression can be given (i.e., hats can be removed from the definition). Here $\omega_n \equiv 2\pi nT$, $n \in \mathbb{Z}$, denotes bosonic Matsubara frequencies. The spectral function is then given by the discontinuity (see, e.g., refs. [25, 26])

$$\rho_V(\omega) = \mathrm{Disc}\left[C_E(-i\omega)\right] \equiv \frac{1}{2i}\Big[C_E(-i[\omega+i0^+]) - C_E(-i[\omega-i0^+])\Big]\,. \tag{2.5}$$

In the following we denote Euclidean four-momenta with capital letters, in particular $Q \equiv (\omega_n,\mathbf{0})$. Moreover, $\sum\!\!\!\!\!\!\int_K \equiv T\sum_{k_n}\mu^{2\epsilon}\int \mathrm{d}^d\mathbf{k}/(2\pi)^d$ stands for a sum-integral over bosonic Matsubara four-momenta, while $\sum\!\!\!\!\!\!\int_{\{P\}}$ signifies a sum-integral over fermionic ones. The space-time dimensionality is denoted by $D \equiv 4-2\epsilon$, and the space dimensionality by $d \equiv 3-2\epsilon$.

[2] For a non-zero total spatial momentum $\mathbf{q}$, with $0 < |\mathbf{q}| \ll M$, the main modification of our results would be a shift of the two-particle threshold from $\omega \approx 2M$ to $\omega \approx 2M + \mathbf{q}^2/4M$.

3. Details of the computation

3.1. Propagators

At a finite temperature T it is not clear, *a priori*, whether the result of the computation will be infrared finite, given that (after analytic continuation) the gluon propagator contains the Bose-enhanced factor $n_{\rm B}(k^0) \approx T/k^0$, for $|k^0| \ll T$. For this reason, we carry out the analysis by using the Hard Thermal Loop resummed [27, 28] form of the gluon propagator, which takes into account Debye screening, and thereby shields (part of) the infrared divergences. Introducing (see, e.g., refs. [25, 26])

$$P^T_{00}(K) \;=\; P^T_{0i}(K) = P^T_{i0}(K) \equiv 0 \;, \quad P^T_{ij}(K) \equiv \delta_{ij} - \frac{k_i k_j}{\mathbf{k}^2} \;, \tag{3.1}$$

$$P^E_{\mu\nu}(K) \;\equiv\; \delta_{\mu\nu} - \frac{K_\mu K_\nu}{K^2} - P^T_{\mu\nu}(K) \;, \tag{3.2}$$

where $K = (k_n, \mathbf{k})$, $k_n = 2\pi n T$, the Euclidean gluon propagator can be written as

$$\langle A^a_\mu(x) A^b_\nu(y)\rangle = \delta^{ab} \sum\!\!\!\!\!\!\int_K e^{iK\cdot(x-y)} \left[\frac{P^T_{\mu\nu}(K)}{K^2 + \Pi_T(K)} + \frac{P^E_{\mu\nu}(K)}{K^2 + \Pi_E(K)} + \frac{\xi\, K_\mu K_\nu}{(K^2)^2} \right] , \tag{3.3}$$

where ξ is a gauge parameter. The projector P^T is transverse both with respect to K and to the four-velocity of the heat bath and, in the static limit, describes colour-magnetic modes; the projector P^E is transverse only with respect to K and, in the static limit, describes colour-electric modes. The self-energies Π_T, Π_E are well-known [27, 28] functions of the form $m_{\rm D}^2\, f(k_n/|\mathbf{k}|)$, where $m_{\rm D} = (N_{\rm c}/3 + N_{\rm f}/6) g T$ is the Debye mass parameter; we will not need their explicit expressions in the following, apart from knowing that f is an even function of its argument and regular on the real axis. The fermion propagator has the free form,

$$\langle \psi(x) \bar\psi(y)\rangle = \sum\!\!\!\!\!\!\int_{\{P\}} e^{iP\cdot(x-y)}\, \frac{-i\not{P} + M_B}{P^2 + M_B^2} \;, \tag{3.4}$$

where M_B is the bare heavy quark mass.

3.2. Contractions

The first step of the computation is to carry out the Wick contractions and the Dirac traces. At 1-loop level, omitting Q-independent terms which are killed by the discontinuity in eq. (2.5), we get

$$= \;\; [Q - \text{indep.}] + 2C_A \sum\!\!\!\!\!\!\int_{\{P\}} \frac{(D-2)Q^2 - 4M^2}{\Delta(P)\Delta(P-Q)} \;. \tag{3.5}$$

Here $C_A \equiv N_{\rm c}$, and

$$\Delta(P) \equiv P^2 + M^2 \;. \tag{3.6}$$

At next-to-leading order (NLO), we have to evaluate the counterterm graph as well as genuine 2-loop graphs. The counterterm graph can be deduced from the 1-loop expression in eq. (3.5), by re-interpreting the mass parameter as the bare one, M_B^2, and then expanding it in terms of the pole mass:

$$M_B^2 = M^2 - \frac{6g^2 C_F M^2}{(4\pi)^2}\left(\frac{1}{\epsilon} + \ln\frac{\bar{\mu}^2}{M^2} + \frac{4}{3}\right) + \mathcal{O}(g^4)\;, \tag{3.7}$$

where $C_F \equiv (N_{\rm c}^2-1)/2N_{\rm c}$, and $\bar{\mu}$ is the scale parameter of the $\overline{\rm MS}$ scheme. This yields

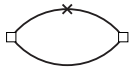

$$\begin{aligned} &= [Q-\text{indep.}] + \frac{24g^2 C_A C_F M^2}{(4\pi)^2}\left(\frac{1}{\epsilon} + \ln\frac{\bar{\mu}^2}{M^2} + \frac{4}{3}\right) \\ &\times \sum\!\!\!\!\!\!\int_{\{P\}} \left[\frac{(D-2)Q^2 - 4M^2}{\Delta^2(P)\Delta(P-Q)} + \frac{2}{\Delta(P)\Delta(P-Q)}\right]. \end{aligned} \tag{3.8}$$

For the genuine 2-loop graphs, we make use of the identities

$$K_\mu P^T_{\mu\nu}(K) = Q_\mu P^T_{\mu\nu}(K) = 0\;, \quad P^T_{\mu\mu}(K) = D-2\;, \quad P_\mu P_\nu P^T_{\mu\nu}(K) = \mathbf{p}^2 - (\mathbf{p}\cdot\hat{\mathbf{k}})^2\;, \tag{3.9}$$

where $\hat{\mathbf{k}} \equiv \mathbf{k}/|\mathbf{k}|$, and the second equality follows from the fact that Q is aligned with the heat bath. We then complete squares in the numerator, and note that

$$\sum\!\!\!\!\!\!\int_{K\{P\}} \frac{Q\cdot K}{[K^2+\Pi(K)]\Delta(P)\Delta(P-Q)\Delta(P-K)\Delta(P-Q-K)} = 0\;, \tag{3.10}$$

as can be shown with the shifts $P\to -P+Q, K\to -K$. Thereby we arrive at

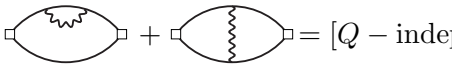

$$\begin{aligned} &= [Q-\text{indep.}] + 4g^2 C_A C_F \sum\!\!\!\!\!\!\int_{K\{P\}} \Bigg\{ \\ &\left(\frac{1}{K^2+\Pi_T} - \frac{1}{K^2+\Pi_E}\right)[\mathbf{p}^2 - (\mathbf{p}\cdot\hat{\mathbf{k}})^2] \times \\ &\qquad \times \left[-\frac{4[(2-D)Q^2+4M^2]}{\Delta^2(P)\Delta(P-Q)\Delta(P-K)} - \frac{2[(2-D)Q^2+4M^2]+4K^2}{\Delta(P)\Delta(P-Q)\Delta(P-K)\Delta(P-Q-K)}\right] \\ &+\frac{D-2}{K^2+\Pi_T}\left[-\frac{2}{\Delta(P)\Delta(P-Q)} + \frac{(2-D)Q^2+4M^2}{\Delta^2(P)\Delta(P-Q)}\right. \\ &\qquad + \frac{2}{\Delta(P)\Delta(P-Q-K)} + \frac{-2(D-2)Q\cdot K + 4K^2}{\Delta(P)\Delta(P-Q)\Delta(P-K)} \\ &\qquad \left. - \frac{[(2-D)Q^2+4M^2]K^2}{\Delta^2(P)\Delta(P-Q)\Delta(P-K)} - \frac{[(6-D)Q^2/2+2M^2]K^2+K^4}{\Delta(P)\Delta(P-Q)\Delta(P-K)\Delta(P-Q-K)}\right] \\ &+\frac{1}{K^2+\Pi_E}\left[-\frac{4[(2-D)Q^2+4M^2]}{\Delta(P)\Delta(P-Q)\Delta(P-K)} + \frac{4[(2-D)Q^2+4M^2]M^2}{\Delta^2(P)\Delta(P-Q)\Delta(P-K)}\right. \\ &\qquad \left. + \frac{(2-D)Q^4 + (8-2D)Q^2M^2 + 8M^4 + [(2-D)Q^2+4M^2]K^2}{\Delta(P)\Delta(P-Q)\Delta(P-K)\Delta(P-Q-K)}\right] \Bigg\}\,. \end{aligned} \tag{3.11}$$

Note that any dependence on the gauge parameter ξ has disappeared; thus $P^E_{\mu\nu}$ could have been replaced with $\delta_{\mu\nu} - P^T_{\mu\nu}$.

3.3. Outline of the subsequent steps

Given eq. (3.11), we need to carry out the Matsubara sums and the spatial momentum integrals. More concretely, the steps (specified in explicit detail for one example in appendix A) are as follows:

- Writing the gluon propagator in a spectral representation, the Matsubara sums $T\sum_{k_n}$ and $T\sum_{\{p_n\}}$ can be carried out exactly in all cases.

- The result after these steps contains many appearances of the Fermi distributions, $n_{\rm F}(E) \equiv 1/[\exp(\beta E)+1]$, where the energy E is that of a heavy quark, $E \geq M$. All such terms are suppressed by at least $e^{-M/T} \ll 1$, and can be omitted.

- The remaining temperature dependence appears as Bose distributions with the gluon energy, $n_{\rm B}(k^0)$. Here the issue is the opposite: in the small energy range, $|k^0| \ll T$, there is an enhancement factor T/k^0, which could lead to infrared divergences. This is an important point, so we devote a separate subsection to it (sec. 3.4). The upshot is that there are *no* infrared divergences at the present order.

- Having verified the absence of infrared divergences, we can forget about the HTL resummation in the gluon propagators, i.e. set $\Pi_T = \Pi_E = 0$ in eq. (3.11), and insert the free spectral function for the gluons. Thereby the integral over the gluon energy k^0 is trivially carried out. (In practice, we first insert the free gluon spectral function, integrate over k^0, and verify the absence of infrared divergences *a posteriori* for each independent ("master") sum-integral separately.)

- The remaining spatial integrals, over $\mathbf{k}$ and $\mathbf{p}$, are effectively three-dimensional (over the absolute values of $\mathbf{k}, \mathbf{p}$ and over the angle between $\mathbf{k}$ and $\mathbf{p}$). Some of them are ultraviolet divergent, and require regularization. The integrals come in two forms, which we call "phase space" and "factorized". We are able to carry out two of the integrations in all cases; for the zero-temperature parts entering the final result, all three integrations are doable [1]–[3], while for the finite-temperature parts an exponentially convergent integral over $k = |\mathbf{k}|$ remains to be carried out numerically.

The results obtained after these steps are listed for all the master sum-integrals appearing in eq. (3.11) in appendix B.

3.4. Absence of infrared divergences

Inserting the free gluon spectral function, which sets $k^0 = k$, into any of the master sum-integrals, there remains an integral over the gluon momentum k to be carried out. In principle this integral could be infrared divergent. This turns out indeed to be the case for the "phase space" and "factorized" parts (for definitions, see appendix A.2) of the integrals separately; in fact, the integrals denoted by S_5^0 and S_6^0 (cf. eqs. (B.20), (B.32)), have logarithmically divergent infrared parts even at zero temperature, which were an issue in the 1970s [2]. However, the infrared divergences were found to cancel in the sum of the phase space and factorized parts. In our case, the logarithmic divergences turn into linear ones, due to the additional factor $n_{\rm B}(k) \approx T/k$; nevertheless, when the phase space and factorized parts are added together, we find that both powerlike and logarithmic divergences cancel, and the integrals become finite, for each master sum-integral separately. This can clearly be seen in eqs. (B.24) and (B.35) for S_5^0 and S_6^0, respectively. The same is true for the integrals denoted by $\hat{S}_5^0, \hat{S}_6^0, \hat{S}_6^2$ (eqs. (B.25), (B.36), (B.45)), appearing in the first term of eq. (3.11) and disappearing if the HTL self-energies are set to zero from the outset. Therefore, we conclude that there are no infrared problems in our observable at the next-to-leading order. (It is to be expected, though, that there are some at higher orders.)

4. Final result

Given the considerations in sec. 3.4, showing the absence of infrared divergences, we are free to set $\Pi_T = \Pi_E = 0$ in eq. (3.11). Noting furthermore that the factorized gluon tadpole reads

$$\sum\!\!\!\!\!\!\int_K \frac{1}{K^2} = \frac{T^2}{12} + \mathcal{O}(\epsilon) \,, \tag{4.1}$$

and employing the notation of appendix B for the sum-integrals $S_i^j(\omega)$, the full result can be written as

$$\begin{aligned}
\rho_V(\omega)\big|_{\rm raw} \;=\; & -4C_A(\omega^2+2M^2)S_1(\omega) + 8g^2C_AC_F\Big\{ \\
& \left[\frac{T^2}{6} - \frac{6M^2}{(4\pi)^2}\left(\frac{1}{\epsilon} + \ln\frac{\bar{\mu}^2}{M^2} + \frac{4}{3}\right)\right]\Big[-S_1(\omega) + (\omega^2+2M^2-\epsilon\,\omega^2)S_2(\omega)\Big] \\
& +2S_3(\omega) - 4(\omega^2+2M^2-\epsilon\,\omega^2)S_4^0(\omega) - 4(1-2\epsilon)S_4^1(\omega) + 4(1-\epsilon)S_4^2(\omega) \\
& +2(\omega^2+2M^2-\epsilon\,\omega^2)\Big[2M^2S_5^0(\omega) - (1-\epsilon)S_5^2(\omega)\Big] - (\omega^4-4M^4)S_6^0(\omega) \\
& +\Big[(2-\epsilon)\omega^2+2\epsilon M^2\Big]S_6^2(\omega) - (1-\epsilon)S_6^4(\omega)\Big\} + \mathcal{O}(\epsilon) \,.
\end{aligned} \tag{4.2}$$

We have set here $\epsilon \to 0$ whenever the master sum-integral that it multiplies is finite.

Now, the explicit thermal correction on the second line of eq. (4.2) has a simple physical meaning: it corresponds to an expansion of the leading-order result through a thermal mass shift [29]

$$M^2 \to M^2 + \frac{g^2 T^2 C_F}{6} \,, \tag{4.3}$$

i.e. $\delta M = g^2 T^2 C_F / 12M$. Note that this term multiplies the function $S_2(\omega) = \theta(\omega - 2M)/[16\pi\omega(\omega^2 - 4M^2)^{1/2}](1 + \mathcal{O}(\epsilon, e^{-\beta M}))$ (cf. eq. (B.6)), which diverges at the threshold, while the sum of all the other terms turns out to remain finite. Thereby the thermal correction would completely dominate the result close enough to the threshold, were it not to be resummed into a mass correction *à la* eq. (4.3). On the other hand, once it has been resummed, this term is in general small: in the range that we are interested in, $g^2 M < T < gM$, it corresponds parametrically to a higher order contribution. Therefore, for simplicity, we drop this term in the following (of course, if desired, it is trivial to include it as an overall mass shift), and reinterpret the result as

$$\begin{aligned}
\rho_V(\omega) \;=\; & -4C_A(\omega^2 + 2M^2)S_1(\omega) + 8g^2 C_A C_F \Big\{ \\
& \left[-\frac{6M^2}{(4\pi)^2}\left(\frac{1}{\epsilon} + \ln\frac{\bar{\mu}^2}{M^2} + \frac{4}{3} \right) \right] \Big[-S_1(\omega) + (\omega^2 + 2M^2 - \epsilon\,\omega^2) S_2(\omega) \Big] \\
& + 2S_3(\omega) - 4(\omega^2 + 2M^2 - \epsilon\,\omega^2) S_4^0(\omega) - 4(1-2\epsilon) S_4^1(\omega) + 4(1-\epsilon) S_4^2(\omega) \\
& + 2(\omega^2 + 2M^2 - \epsilon\,\omega^2) \Big[2M^2 S_5^0(\omega) - (1-\epsilon) S_5^2(\omega) \Big] - (\omega^4 - 4M^4) S_6^0(\omega) \\
& + \Big[(2-\epsilon)\omega^2 + 2\epsilon M^2 \Big] S_6^2(\omega) - (1-\epsilon) S_6^4(\omega) \Big\} + \mathcal{O}(\epsilon) \,.
\end{aligned} \tag{4.4}$$

Nevertheless, it is perhaps appropriate to stress that only the part of the thermal correction multiplying the function $S_2(\omega)$ can be unambiguously resummed on the grounds that the result would otherwise diverge at the threshold, while the term $\sim T^2 S_1(\omega)$ could in principle be kept explicit, and would then have an $\mathcal{O}(1)$ effect on the thermal part of the result.

Inserting the explicit expressions for the functions $S_i^j(\omega)$ from appendix B into eq. (4.4), the final result for the vacuum part becomes

$$\begin{aligned}
\rho_V(\omega)|^{\rm vac} \;=\; & -\theta(\omega - 2M) \frac{C_A(\omega^2 - 4M^2)^{\frac{1}{2}}(\omega^2 + 2M^2)}{4\pi\omega} + \theta(\omega - 2M) \frac{8g^2 C_A C_F}{(4\pi)^3 \omega^2} \Big\{ \\
& (4M^4 - \omega^4) L_2\!\left(\frac{\omega - \sqrt{\omega^2 - 4M^2}}{\omega + \sqrt{\omega^2 - 4M^2}} \right) + (7M^4 + 2M^2\omega^2 - 3\omega^4) \,\mathrm{acosh}\!\left(\frac{\omega}{2M} \right) \\
& + \omega(\omega^2 - 4M^2)^{\frac{1}{2}} \left[(\omega^2 + 2M^2) \ln\frac{\omega(\omega^2 - 4M^2)}{M^3} - \frac{3}{8}(\omega^2 + 6M^2) \right] \Big\} + \mathcal{O}(\epsilon, g^4) \,,
\end{aligned} \tag{4.5}$$

where the function L_2 is defined as

$$L_2(x) \equiv 4\,\mathrm{Li}_2(x) + 2\,\mathrm{Li}_2(-x) + [2\ln(1-x) + \ln(1+x)]\ln x\;. \tag{4.6}$$

The result in eq. (4.5) agrees with the classic result from the literature [1]–[3]. The thermal correction, in turn, reads,

$$\begin{aligned}
\rho_V(\omega)|^T \;=\; & \frac{8g^2C_AC_F}{(4\pi)^3\omega^2}\int_0^\infty \mathrm{d}k\,\frac{n_{\mathrm{B}}(k)}{k}\Bigg\{ \\
& \theta(\omega)\,\theta\Big(k-\frac{4M^2-\omega^2}{2\omega}\Big)\Bigg[2\omega^2k^2\sqrt{1-\frac{4M^2}{\omega(\omega+2k)}} \\
& \quad +(\omega^2+2M^2)\sqrt{\omega(\omega+2k)}\sqrt{\omega(\omega+2k)-4M^2} \\
& \quad -2\Big(\omega^4-4M^4+2\omega k(\omega^2+2M^2)+2\omega^2k^2\Big)\,\mathrm{acosh}\sqrt{\frac{\omega(\omega+2k)}{4M^2}}\Bigg] \\
+ \;\; & \theta(\omega-2M)\,\theta\Big(\frac{\omega^2-4M^2}{2\omega}-k\Big)\Bigg[2\omega^2k^2\sqrt{1-\frac{4M^2}{\omega(\omega-2k)}} \\
& \quad +(\omega^2+2M^2)\sqrt{\omega(\omega-2k)}\sqrt{\omega(\omega-2k)-4M^2} \\
& \quad -2\Big(\omega^4-4M^4-2\omega k(\omega^2+2M^2)+2\omega^2k^2\Big)\,\mathrm{acosh}\sqrt{\frac{\omega(\omega-2k)}{4M^2}}\Bigg] \\
+ \;\; & \theta(\omega-2M)\Bigg[-2(\omega^2+2M^2)\,\omega\sqrt{\omega^2-4M^2} \\
& \quad +4\Big(\omega^4-4M^4+2\omega^2k^2\Big)\,\mathrm{acosh}\Big(\frac{\omega}{2M}\Big)\Bigg]\Bigg\} + \mathcal{O}(e^{-\beta M},g^4)\;,
\end{aligned} \tag{4.7}$$

where we have restricted to $\omega > 0$ ($\omega < 0$ follows from antisymmetry, $\rho_V(-\omega) = -\rho_V(\omega)$). Eq. (4.7) is our main result.

A numerical evaluation of eq. (4.7), compared with the vacuum part in eq. (4.5), is shown in fig. 1. We note that even though the thermal part is not exponentially suppressed for $\omega > 2M$, it still only amounts to a small correction at phenomenologically interesting temperatures. On the other hand, the thermal part does possess the new qualitative feature that the result is non-zero below the threshold as well, where it is then the dominant effect; this can be traced back to reactions where a heavy quark and anti-quark annihilate into a gluon remaining inside the thermal medium, and a photon escaping from it.

As an amusing remark, we note that while the next-to-leading order vacuum part is discontinuous at the threshold, the next-to-leading order thermal part appears to be continuous. A similar pattern holds also for the scalar channel (fig. 6): then the next-to-leading order vacuum part is continuous, while the next-to-leading order thermal part appears to have a continuous first derivative. These features are perhaps a manifestation of the fact that a non-zero temperature in general "smoothens" the spectral function; in a resummed framework,

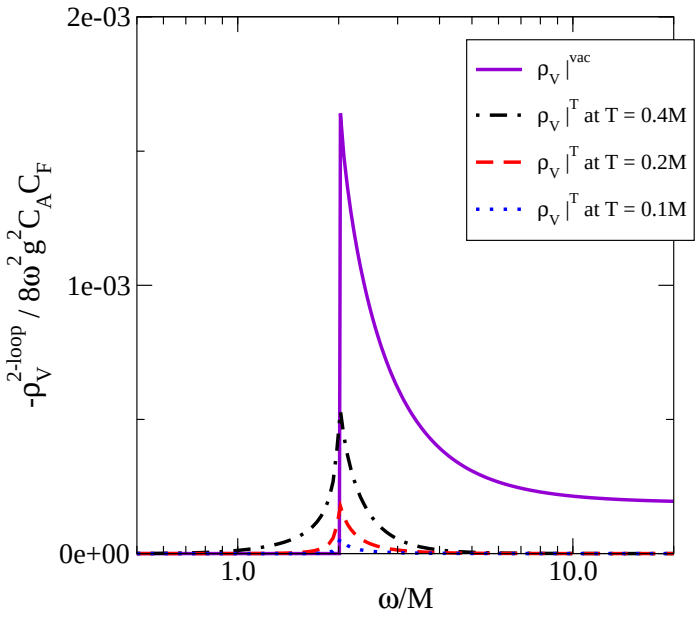

Figure 1: The vacuum and thermal parts of the next-to-leading order correction in the vector channel, normalized by dividing with $-8\omega^2 g^2 C_A C_F$. The vacuum part remains finite for $\omega \to \infty$ (in units of the figure, its asymptotic value is $3/512\pi^3$), while the thermal part disappears fast for $\omega/M \gg 1$.

it may then not be surprising if any resonance peak of the vacuum result should disappear from the spectral function at high enough temperatures.

To summarize, the characteristic feature of fig. 1 is a significant "threshold enhancement", due mostly to the vacuum part at $T \ll M$. Within perturbation theory, this is to be interpreted as a first term of a series which, when summed to all orders, builds up possible quarkonium resonance peaks at $\omega < 2M$. At the same time, the result of a resummed computation (to be discussed in more detail at the beginning of the next section) should extrapolate towards the perturbative one at some $\omega > 2M$.

5. Phenomenological implications

We would now like to combine our result with that obtained within an NRQCD [30, 31] and PNRQCD [32, 33] inspired resummed framework in ref. [8]. In order to do this, we need to pay attention to the correct normalization of the resummed result. In fact, the well-known (vacuum) normalization factor can be read off from eq. (4.5): denoting

$$v \equiv \frac{\sqrt{\omega^2 - 4M^2}}{\omega}\,, \tag{5.1}$$

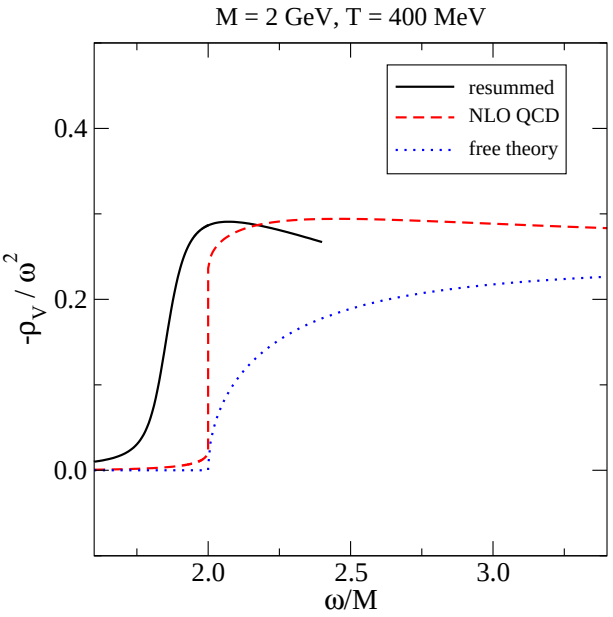

Figure 2: A comparison of the near-threshold "resummed" result of ref. [8], matched to the "NLO QCD" expression of the present paper through an overall normalization factor, as discussed in the text. The difference of the NLO QCD result and the free theory result contains both the vacuum part and the thermal part; the magnitude of the latter is reflected by how much the curve deviates from zero below the threshold.

the leading order vacuum expression can be expanded near the threshold as

$$-\frac{\rho_V(\omega)}{\omega^2}\bigg|_{\rm LO} = \theta(\omega-2M)\left[\frac{3C_A v}{8\pi}+\mathcal{O}(v^3)\right], \tag{5.2}$$

while the next-to-leading order vacuum result becomes

$$-\frac{\rho_V(\omega)}{\omega^2}\bigg|_{\rm NLO} = 8g^2C_AC_F\theta(\omega-2M)\left[\frac{3}{512\pi}-\frac{3v}{64\pi^3}+\mathcal{O}(v^2)\right]. \tag{5.3}$$

Since radiative corrections within a non-relativistic framework always contain a power of v, it is possible to account for the second term in eq. (5.3), equalling $-g^2C_F/\pi^2$ times the leading term in eq. (5.2), only by a multiplicative correction of the current,[3]

$$\mathcal{J}^\mu_{\rm QCD} = \mathcal{J}^\mu_{\rm NRQCD}\left(1-\frac{g^2C_F}{2\pi^2}+...\right). \tag{5.4}$$

In principle the coupling here should be evaluated at the scale $\sim M$ [35], but in practice our resolution is low enough that we follow a simpler recipe (cf. next paragraph). In any case,

[3]The same relation is valid both for NRQCD and PNRQCD [34].

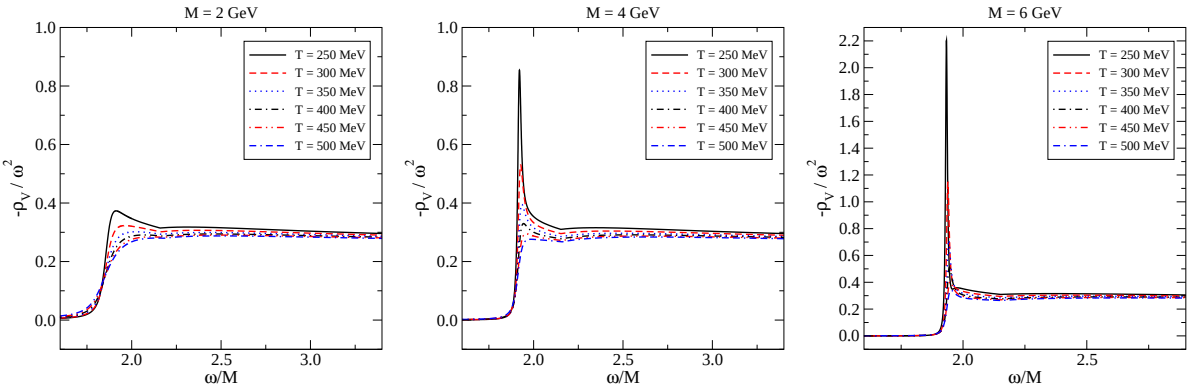

Figure 3: The phenomenologically assembled vector channel spectral function $\rho_V(\omega)$, in units of $-\omega^2$, for $M = 2, 4, 6$ GeV (from left to right). To the order considered, M is the heavy quark pole mass. Note that for better visibility, the axis ranges are different in the rightmost figure.

the normalization factor is numerically significant, and its precise treatment plays a role; we actually do not impose it exactly, but rather search for a value minimizing the squared difference of the two results in the range $(\omega - 2M)/M = 0.0 - 0.4$, thereby also accounting for thermal corrections. This results in a normalization factor in the range $0.7 - 0.9$, which indeed is the same ballpark as suggested by (the square of) eq. (5.4), given our choice of g^2 (cf. next paragraph). The "interpolated", or rather "assembled" result, is subsequently defined as $\rho_V^{(\mathrm{assembled})} \equiv \max(\rho_V^{(\mathrm{QCD})}, \rho_V^{(\mathrm{resummed})})$. An example for how the interpolation works in practice is shown in fig. 2.

As far as the value of g^2 goes, no systematic choice is possible in the absence of NNLO computations at finite temperature. We follow here a purely phenomenological recipe, whereby g^2 is taken from another context where a sufficient level has been reached [36], and take [37]

$$g^2 \simeq \frac{8\pi^2}{9\ln(9.082\,T/\Lambda_{\overline{\mathrm{MS}}})}\,, \qquad \text{for } N_{\mathrm{c}} = N_{\mathrm{f}} = 3\,. \tag{5.5}$$

We also fix $\Lambda_{\overline{\mathrm{MS}}} \simeq 300$ MeV to be compatible with ref. [8]. It should be obvious that the subsequent results contain unknown uncertainties; still, the situation could in principle be systematically improved upon through higher order computations.

The resulting full spectral function is shown in figs. 3, 4 for various masses and temperatures, as a function of ω. The corresponding dilepton production rate from eq. (2.2) is shown in fig. 5. Compared with the results in ref. [8], the absolute magnitude of the rate has decreased by about 10 – 30%, due to the inclusion of the normalization factor. We should again stress that particularly the charmonium case contains large uncertainties, and our results are to be trusted on the qualitative level only.

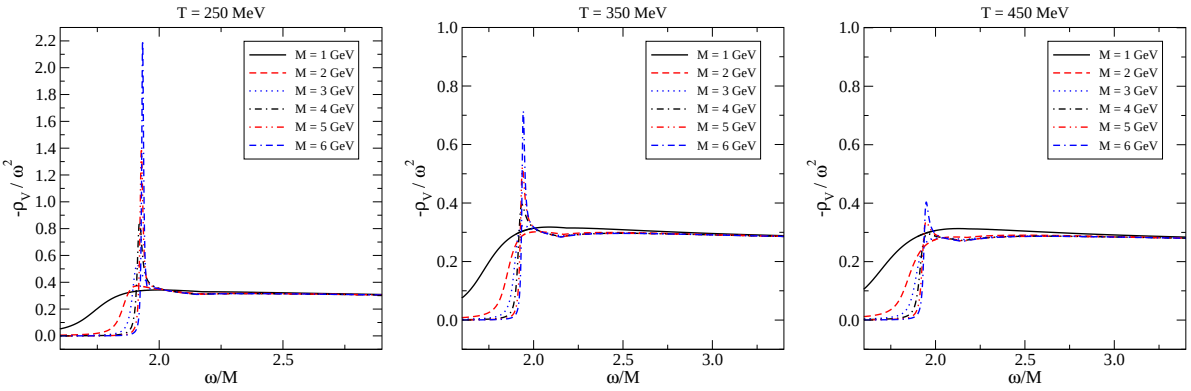

Figure 4: The phenomenologically assembled vector channel spectral function $\rho_V(\omega)$, in units of $-\omega^2$, for $T = 250, 350, 450$ MeV (from left to right). To the order considered, M is the heavy quark pole mass. Note that for better visibility, the axis ranges are different in the leftmost figure.

6. Conclusions

The purpose of this paper has been to compute the heavy quark contribution to the spectral function of the electromagnetic current at next-to-leading order in thermal QCD. The result consists of a well-known vacuum part, eq. (4.5), and a new thermal part, eq. (4.7). The thermal part is illustrated numerically in fig. 1 in comparison with the vacuum part.

The thermal corrections in our result arise exclusively from the gluons with which the heavy quarks interact. Although these contributions are not exponentially suppressed, they turn out to be power-suppressed at large energies $\omega \gg 2M$: their general magnitude is $\mathcal{O}(g^2T^2)$, and given that $T < gM$ is the phenomenologically interesting temperature range (cf. eq. (2.3)), they can in principle be omitted in comparison with the next-to-leading order zero-temperature corrections, of $\mathcal{O}(g^2M^2)$. This also means that the asymptotic behaviour of the spectral function, needed as input for lattice studies, could (in the continuum limit) be extracted from the well-studied zero-temperature computations (see, e.g., ref [24]). At zero temperature the next-to-leading order correction could, perhaps, even be worked out at a finite lattice spacing.

On the other hand, decreasing the energy towards the threshold, the thermal corrections become increasingly important. In fact, at next-to-leading order, the vacuum spectral function vanishes at $\omega < 2M$, while the thermal correction stays finite. The result emerges from phase space integrals associated with the energy constraint $\delta(\omega + k - E_1 - E_2)$, where ω is the photon energy; k is the gluon energy; and E_1, E_2 are the energies of a heavy quark and anti-quark. Graphically, the process corresponds to the annihilation of quarkonium into a gluon and a photon, the former of which remains within the thermal medium. Since large values of k are Boltzmann suppressed, the thermal corrections are substantial only for $|\omega - 2M| \lesssim T$.

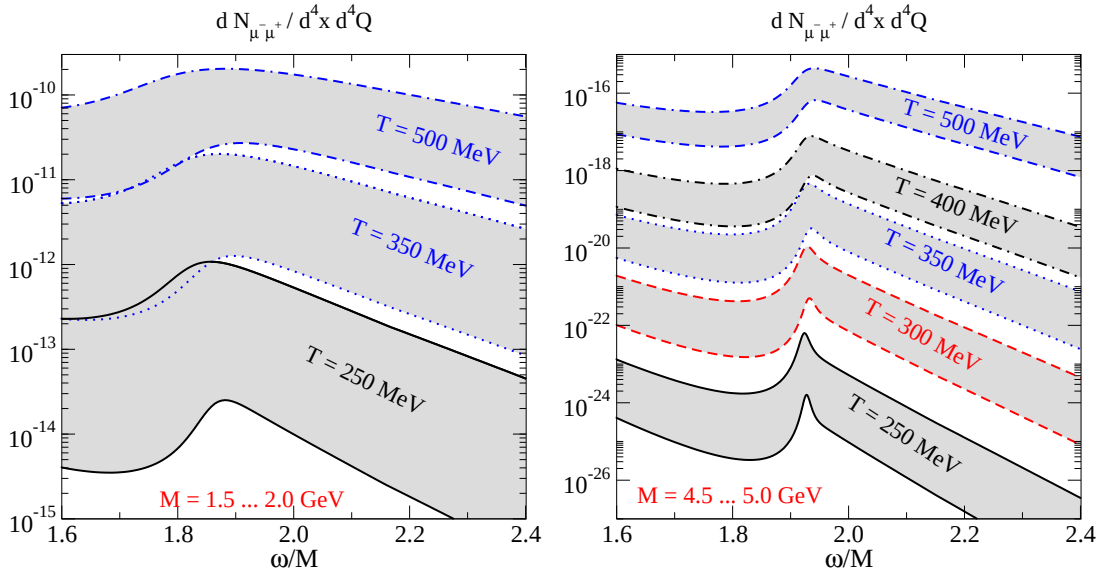

Figure 5: The physical dilepton production rate, eq. (2.2), from charmonium (left) and bottomonium (right), as a function of the energy, for various temperatures. The mass M corresponds to the pole mass, and is subject to uncertainties of several hundred MeV; we use the intervals 1.5...2.0 GeV and 4.5...5.0 GeV to illustrate the uncertainties. The low mass corresponds to the upper edge of each band. Compared with ref. [8], the main change is a 10 – 30% reduction of the overall magnitude.

Combining our new results, valid far enough away from the threshold, with previously determined resummed expressions, valid close to the threshold, we have subsequently assembled phenomenological estimates for the spectral function in a macroscopic energy range (figs. 3, 4). The corresponding dilepton production rate is shown in fig. 5. Analogous results and plots for the spectral function in the scalar channel have been given in appendix C. The computations of the present paper play an important role in these plots particularly in that they fix the overall normalization of the assembled curves. We hope that these results can eventually be incorporated in a simulation including an expanding and cooling thermal fireball, which would then allow for a direct comparison with the dilepton production rate measured in heavy ion collision experiments.

We note, finally, that we have restricted to $\omega > 0$ in this paper. There is a lot of interesting structure in the vector channel spectral function also around $\omega \approx 0$, related to the heavy quark diffusion coefficient. However, that structure is suppressed by $\exp(-\beta M)$, and a non-trivial result also only arises at the order $\mathcal{O}(\alpha_s^2)$ [38], so that our present computation at $\mathcal{O}(\alpha_s)$ cannot add anything to the known results [39].

Acknowledgements

We thank S. Caron-Huot, D. Bödeker and Y. Schröder for useful discussions, and are grateful to the BMBF for financial support under project *Hot Nuclear Matter from Heavy Ion Collisions and its Understanding from QCD*.

Appendix A. Intermediate steps for a master sum-integral

We elaborate in this appendix on the steps outlined in sec. 3.3. The starting point is the expression in eq. (3.11).

A.1. Matsubara sums and the spectral function

The first step is to carry out the Matsubara sums $T\sum_{k_n}$, $T\sum_{\{p_n\}}$. The sum $T\sum_{k_n}$ is complicated by the appearance of the functions Π_E, Π_T in the gluon propagators. The reason for their introduction was that there could in principle be infrared divergences associated with the gluons; in the Euclidean formalism, these would come from small spatial momenta $\mathbf{k}$ for the Matsubara zero mode $k_n = 0$, and could then be regulated by the fact that $\Pi_E(0,\mathbf{k}) = m_{\rm D}^2 > 0$. Our strategy in the following will be to *assume* that there are no infrared divergences, whereby we can set $\Pi_T = \Pi_E = 0$; the absence of divergences will be verified *a posteriori*. Nevertheless, it has still been important to keep $\Pi_E \neq \Pi_T$ in eq. (3.11), because it could happen that the structure multiplied by $1/(K^2+\Pi_T) - 1/(K^2+\Pi_E)$, which vanishes in the free limit, contains infrared sensitive parts which do not completely cancel against each other in the presence of $\Pi_E \neq \Pi_T$.

In order to allow for an eventual introduction of Π_E and Π_T, we write for the moment the gluon propagators in the spectral representation,

$$\frac{1}{K^2+\Pi(K)} = \int_{-\infty}^{\infty} \frac{{\rm d}k^0}{\pi} \frac{\rho(k^0,\mathbf{k})}{k^0 - ik_n} \,, \tag{A.1}$$

and carry out the Matsubara sum $T\sum_{k_n}$ with the kernel $1/(k^0 - ik_n)$. In the free case, when the spectral function reads

$$\rho_{\rm free}(k^0,\mathbf{k}) = \frac{\pi}{2k}\Big[\delta(k^0-k) - \delta(k^0+k)\Big] \,, \tag{A.2}$$

with $k \equiv |\mathbf{k}|$, the whole procedure is obviously just a rewriting of the decomposition

$$\frac{1}{k_n^2+k^2} = \frac{1}{2k}\left[\frac{1}{k-ik_n} + \frac{1}{k+ik_n}\right] . \tag{A.3}$$

Note that the procedure is rather versatile and could also be interpreted as

$$
\begin{aligned}
\frac{1}{K^2+\Pi(K)} &= \left[1-\frac{\Pi(K)}{K^2+\Pi(K)}\right]\frac{1}{K^2} \qquad \text{(A.4)}\\
&= \int_{-\infty}^{\infty}\frac{\mathrm{d}k^0}{\pi}\left\{\frac{\rho_{\rm free}(k^0,\mathbf{k})}{k^0-ik_n}+\frac{\bar\rho(k^0,\mathbf{k})}{2k}\left(\frac{1}{k^0+ik_n}-\frac{1}{k+ik_n}+\frac{1}{k^0-ik_n}-\frac{1}{k-ik_n}\right)\frac{1}{k-k^0}\right\} ,
\end{aligned}
$$

where $\bar\rho(k^0,\mathbf{k})$ is the spectral function corresponding to $-\Pi/(K^2+\Pi)$, and we made use of the spectral function's antisymmetry in $k^0\to -k^0$. All the sums over k_n are now with the same kernel as the one following from eq. (A.1). The representation in eq. (A.4) would be relevant for Π_E, in which case ρ_E would have a pole at $k^0=k$ [25].

After this lengthy introduction, we are ready to carry out the sums. We describe the procedure in some detail for one of the master sum-integrals appearing in eq. (3.11); for the others, the results are listed in appendix B.

The case we choose to consider in detail is

$$
S_4^0(\omega)\equiv \mathrm{Disc}\left[\int_{-\infty}^{\infty}\frac{\mathrm{d}k^0}{\pi}\,\mathop{\Sigma\!\!\!\!\!\!\int}_{K\{P\}}\frac{\rho(k^0,\mathbf{k})}{k^0-ik_n}\frac{1}{\Delta(P)\Delta(P-Q)\Delta(P-K)}\right]_{Q=(\omega_n\to -i\omega,\mathbf{0})} . \qquad \text{(A.5)}
$$

Denoting

$$
E_p\equiv\sqrt{\mathbf{p}^2+M^2}\ , \quad E_{p-k}\equiv\sqrt{(\mathbf{p}-\mathbf{k})^2+M^2}\ , \qquad \text{(A.6)}
$$

we can rewrite the sums as

$$
\begin{aligned}
& T\sum_{k_n}T\sum_{\{p_n\}}\frac{1}{[k^0-ik_n][p_n^2+E_p^2][(p_n-\omega_n)^2+E_p^2][(p_n-k_n)^2+E_{p-k}^2]}\\
&= T^4\sum_{k_n}\sum_{\{p_n\}}\sum_{\{r_n\}}\sum_{\{s_n\}}\frac{\beta\delta_{r_n-p_n+\omega_n,0}\,\beta\delta_{s_n-p_n+k_n,0}}{[k^0-ik_n][p_n^2+E_p^2][r_n^2+E_p^2][s_n^2+E_{p-k}^2]}\\
&= \int_0^\beta\!\mathrm{d}\tau\int_0^\beta\!\mathrm{d}\sigma\, e^{i\omega_n\tau}T^4\sum_{k_n}\sum_{\{p_n\}}\sum_{\{r_n\}}\sum_{\{s_n\}}\frac{e^{ik_n\sigma}}{k^0-ik_n}\frac{e^{-ip_n(\tau+\sigma)}}{p_n^2+E_p^2}\frac{e^{ir_n\tau}}{r_n^2+E_p^2}\frac{e^{is_n\sigma}}{s_n^2+E_{p-k}^2}\ , \qquad \text{(A.7)}
\end{aligned}
$$

where in the last step we used a representation of the Kronecker delta-function, $\beta\delta_{t_n,0}=\int_0^\beta\mathrm{d}\tau\, e^{it_n\tau}$. The sums have factorized and can now be carried out:

$$
T\sum_{k_n}\frac{e^{ik_n\sigma}}{k^0-ik_n} = n_{\rm B}(k^0)e^{(\sigma\,\mathrm{mod}\,\beta)k^0}\ , \quad 0<\sigma\,\mathrm{mod}\,\beta<\beta\ , \qquad \text{(A.8)}
$$

$$
T\sum_{\{r_n\}}\frac{e^{\pm ir_n\tau}}{r_n^2+E_p^2} = \frac{n_{\rm F}(E_p)}{2E_p}\left[e^{(\beta-|\tau\,\mathrm{mod}\,2\beta|)E}-e^{|\tau\,\mathrm{mod}\,2\beta|E}\right] , \quad -\beta\le\tau\,\mathrm{mod}\,2\beta\le\beta\ , \qquad \text{(A.9)}
$$

where $n_{\rm F}(\omega)\equiv 1/[\exp(\beta\omega)+1]$ and $n_{\rm B}(\omega)\equiv 1/[\exp(\beta\omega)-1]$.[4] The subsequent integrals over τ and σ are elementary; we simply need to split $\int_0^\beta\mathrm{d}\sigma=\int_0^{\beta-\tau}\mathrm{d}\sigma+\int_{\beta-\tau}^\beta\mathrm{d}\sigma$, and note that in

[4] The sum in eq. (A.8) is discontinuous at $\sigma=0\,\mathrm{mod}\,\beta$, and defining its value at the discontinuity requires care; although of no importance in the present context, we note that the expression with the correct antisymmetry in k^0 corresponds to the "average", $n_{\rm B}(k^0)(1+e^{\beta k^0})/2=n_{\rm B}(k^0)+\frac{1}{2}$.

the latter range, $|\tau+\sigma \bmod 2\beta| = 2\beta-\tau-\sigma$. Setting $e^{i\omega_n\beta}\equiv 1$ after the integrations, the ω_n-dependence of the result appears only in structures like $1/(i\omega_n+\sum_i E_i)$, and we can read off the discontinuity:

$$\mathrm{Disc}\left[\frac{1}{i\omega_n+\sum_i E_i}\right]_{\omega_n\to -i\omega} = -\pi\delta(\omega+\sum_i E_i)\;. \tag{A.10}$$

Implementing these steps in practice, and restricting the k^0-integral to positive values by making use of the antisymmetry of $\rho(k^0,\mathbf{k})$, we arrive at

$$\begin{aligned} S_4^0(\omega) \;=\; & \int_0^\infty \frac{\mathrm{d}k^0}{\pi}\int_{\mathbf{k},\mathbf{p}}\rho(k^0,\mathbf{k})\frac{\pi}{4E_pE_{p-k}}\Big\{ \\ & \frac{1}{2E_p}\Big[\delta(\omega-2E_p)-\delta(\omega+2E_p)\Big](1-2n_{\mathrm{F}1})\,\times \\ & \times\Big[(\Delta_{++}^{-1}+\Delta_{-+}^{-1})(1+n_{\mathrm{B}0}-n_{\mathrm{F}2})-(\Delta_{--}^{-1}+\Delta_{+-}^{-1})(n_{\mathrm{B}0}+n_{\mathrm{F}2})\Big] \\ & -\Big[\delta(\omega-\Delta_{++})-\delta(\omega+\Delta_{++})\Big]\Delta_{++}^{-1}\Delta_{-+}^{-1}\Big[(1+n_{\mathrm{B}0})(1-n_{\mathrm{F}1}-n_{\mathrm{F}2})+n_{\mathrm{F}1}n_{\mathrm{F}2}\Big] \\ & -\Big[\delta(\omega-\Delta_{--})-\delta(\omega+\Delta_{--})\Big]\Delta_{--}^{-1}\Delta_{+-}^{-1}\Big[-n_{\mathrm{B}0}(1-n_{\mathrm{F}1}-n_{\mathrm{F}2})+n_{\mathrm{F}1}n_{\mathrm{F}2}\Big] \\ & -\Big[\delta(\omega-\Delta_{+-})-\delta(\omega+\Delta_{+-})\Big]\Delta_{--}^{-1}\Delta_{+-}^{-1}\Big[n_{\mathrm{B}0}n_{\mathrm{F}1}-(1+n_{\mathrm{B}0})n_{\mathrm{F}2}+n_{\mathrm{F}1}n_{\mathrm{F}2}\Big] \\ & -\Big[\delta(\omega-\Delta_{-+})-\delta(\omega+\Delta_{-+})\Big]\Delta_{++}^{-1}\Delta_{-+}^{-1}\Big[n_{\mathrm{B}0}n_{\mathrm{F}2}-(1+n_{\mathrm{B}0})n_{\mathrm{F}1}+n_{\mathrm{F}1}n_{\mathrm{F}2}\Big]\Big\}\;. \end{aligned} \tag{A.11}$$

To simplify the expression somewhat, we have introduced the shorthands

$$\Delta_{\sigma\tau}\equiv k^0+\sigma E_p+\tau E_{p-k}\;,\quad \sigma,\tau=\pm\;, \tag{A.12}$$

$$n_{\mathrm{B}0}\equiv n_{\mathrm{B}}(k^0)\;,\quad n_{\mathrm{F}1}\equiv n_{\mathrm{F}}(E_p)\;,\quad n_{\mathrm{F}2}\equiv n_{\mathrm{F}}(E_{p-k})\;. \tag{A.13}$$

Note that the result in eq. (A.11) is antisymmetric in $\omega\to-\omega$, as must be the case.

Inspecting eq. (A.11), we note the appearance of structures in the denominator, Δ_{+-} etc, which look like they might vanish for some $\mathbf{k},\mathbf{p}$. In fact, in one of the other master sum-integrals, even the structure $1/(E_{p-k}-E_p)$ appears, which certainly vanishes, for $2\mathbf{p}\cdot\mathbf{k}=\mathbf{k}^2$. It can be verified, however, that such poles always cancel between the various types of terms in the expression, and do not hinder the actual integration. (If integration variables are changed in a subset of the expression, $\mathbf{p}\to-\mathbf{p}+\mathbf{k}$, to remove an apparent symmetry in $E_p\leftrightarrow E_{p-k}$, then such terms do not in general cancel any more; nevertheless their contribution remains finite and correct if the poles are interpreted as principal values.)

A.2. Spatial momentum integrals

The result so far, eq. (A.11), contains integrals with two types of delta-functions: ones with $\delta(\omega\pm 2E_p)$, which we call "factorized" (fz) integrals, because the gluon momentum $\mathbf{k}$ does

not appear inside the δ-functions; and ones with more complicated δ-functions, which we call "phase space" (ps) integrals. In both cases, our strategy is to first carry out the integral over the quark momentum $p \equiv |\mathbf{p}|$ and over the angle between $\mathbf{p}$ and $\mathbf{k}$; the integral over the gluon momentum $k \equiv |\mathbf{k}|$ is left for later (it is this integral which could potentially suffer from infrared divergences).

We start by considering the phase space integrals, which are ultraviolet finite, so that we can set $d = 3$. In order to simplify the task, we ignore from now on terms suppressed by $\exp(-\beta M) \ll 1$. This means that all appearances of $n_{\rm F}(E_p)$ and $n_{\rm F}(E_{p-k})$ can be omitted. Furthermore, restricting to $\omega > 0$, we note that the delta-function $\delta(\omega - \Delta_{--}) = \delta(\omega + E_p + E_{p-k} - k^0)$ can only be realized for $k^0 > 2M$, and will then lead to an exponentially small contribution due to the appearance of the Bose distribution $n_{\rm B}(k^0)$. The delta-function $\delta(\omega + \Delta_{++}) = \delta(\omega + k^0 + E_p + E_{p-k})$ does not get realized at all. Thereby only two of the eight delta-functions in eq. (A.11) remain non-zero, and the integral simplifies to

$$S_4^0(\omega)\big|_{\rm ps} \;=\; \int_0^\infty \frac{{\rm d}k^0}{\pi} \int \frac{{\rm d}^3\mathbf{k}}{(2\pi)^3}\, \rho(k^0,\mathbf{k}) \int \frac{{\rm d}^3\mathbf{p}}{(2\pi)^3} \frac{\pi}{E_p E_{p-k}} \Big\{ \\ \delta(\omega - k^0 - E_p - E_{p-k})[1 + n_{\rm B}(k^0)]\phi(k^0) + \delta(\omega + k^0 - E_p - E_{p-k}) n_{\rm B}(k^0) \phi(-k^0) \Big\} \,, \tag{A.14}$$

where

$$\phi(k^0) \equiv \frac{-1}{4(k^0 + E_p + E_{p-k})(k^0 - E_p + E_{p-k})} \,. \tag{A.15}$$

Fixing $\mathbf{k}$ and denoting $z \equiv -\mathbf{p}\cdot\mathbf{k}/pk$, so that $E_{p-k} = \sqrt{p^2 + k^2 + 2pkz + M^2}$, we can change integration variables from p, z to E_p, E_{p-k}:

$$\int {\rm d}^3\mathbf{p} = 2\pi \int_0^\infty {\rm d}p\, p^2 \int_{-1}^{+1} {\rm d}z = 2\pi \int_M^\infty {\rm d}E_p \int_{E_{p-k}^-}^{E_{p-k}^+} {\rm d}E_{p-k} \frac{E_p E_{p-k}}{k} \,, \tag{A.16}$$

where $E_{p-k}^\pm \equiv \sqrt{p^2 \pm 2pk + k^2 + M^2}$. The hard task is to figure out when the δ-functions get realized. For $\delta(\omega - k^0 - E_p - E_{p-k})$ this happens provided that $E_{p-k}^- < \omega - k^0 - E_p < E_{p-k}^+$, which leads to

$$\omega > 2M \,, \quad k^0 < \omega - 2M \,, \quad k < \sqrt{(\omega - k^0)^2 - 4M^2} \,, \tag{A.17}$$

$$\frac{\omega - k^0}{2} - \frac{k}{2}\sqrt{1 - \frac{4M^2}{(\omega - k^0)^2 - k^2}} < E_p < \frac{\omega - k^0}{2} + \frac{k}{2}\sqrt{1 - \frac{4M^2}{(\omega - k^0)^2 - k^2}} \,. \tag{A.18}$$

In the case of the free gluon spectral function, with $k^0 = k$, these simplify to

$$\omega > 2M \,, \quad k < \frac{\omega^2 - 4M^2}{2\omega} \,, \tag{A.19}$$

$$\frac{\omega - k}{2} - \frac{k}{2}\sqrt{1 - \frac{4M^2}{\omega(\omega - 2k)}} < E_p < \frac{\omega - k}{2} + \frac{k}{2}\sqrt{1 - \frac{4M^2}{\omega(\omega - 2k)}} \,. \tag{A.20}$$

For $\delta(\omega + k^0 - E_p - E_{p-k})$, we simply need to set $k^0 \to -k^0$ in eqs. (A.17), (A.18); putting subsequently $k^0 = k$, the explicit expressions read

$$\omega > 0\,, \quad k > \max\biggl(0, \frac{4M^2 - \omega^2}{2\omega}\biggr)\,, \tag{A.21}$$

$$\frac{\omega + k}{2} - \frac{k}{2}\sqrt{1 - \frac{4M^2}{\omega(\omega + 2k)}} < E_p < \frac{\omega + k}{2} + \frac{k}{2}\sqrt{1 - \frac{4M^2}{\omega(\omega + 2k)}}\,. \tag{A.22}$$

Note also that the function ϕ evaluates to $-1/[4\omega(\omega - 2E_p)]$ after integration over E_{p-k}, for both delta functions in eq. (A.14).

Inserting the free gluon spectral function from eq. (A.2) and using the simplified formulae from eqs. (A.19)–(A.22), the integrals over E_{p-k} and E_p can now be carried out. For the thermal part, i.e. the one proportional to $n_{\rm B0}$, this yields

$$\begin{aligned} S_4^0(\omega)\bigr|_{\rm ps}^T \;=\; & \frac{1}{(4\pi)^3\omega}\biggl\{\int_0^\infty {\rm d}k\, n_{\rm B}(k)\biggl[\theta(\omega)\,\theta\Bigl(k - \frac{4M^2 - \omega^2}{2\omega}\Bigr)\,{\rm acosh}\sqrt{\frac{\omega(\omega + 2k)}{4M^2}} \\ & - \theta(\omega - 2M)\,\theta\Bigl(\frac{\omega^2 - 4M^2}{2\omega} - k\Bigr)\,{\rm acosh}\sqrt{\frac{\omega(\omega - 2k)}{4M^2}}\,\biggr]\biggr\} + \mathcal{O}(e^{-\beta M})\,. \end{aligned} \tag{A.23}$$

The vacuum part, on the other hand, is given by the latter row of eq. (A.23), but just without the function $n_{\rm B}(k)$; then the final k-integral is doable as well, and we end up with

$$S_4^0(\omega)\bigr|_{\rm ps}^{\rm vac} \;=\; \frac{1}{(4\pi)^3}\theta(\omega - 2M)\biggl[\frac{(\omega^2 - 4M^2)^{\frac{1}{2}}}{4\omega} + \frac{2M^2 - \omega^2}{2\omega^2}\,{\rm acosh}\Bigl(\frac{\omega}{2M}\Bigr)\biggr]\,. \tag{A.24}$$

Consider next the factorized integrals, i.e. the first term inside the curly brackets in eq. (A.11). Again we start by integrating over p, z, and leave the integration over k for later. This time it is useful to view z as part of the $\mathbf{k}$-integral, i.e.

$$\mu^{2\epsilon}\int\frac{{\rm d}^d\mathbf{k}}{(2\pi)^d} = \frac{4\mu^{2\epsilon}}{(4\pi)^{\frac{d+1}{2}}\Gamma(\frac{d-1}{2})}\int_0^\infty {\rm d}k\, k^{d-1}\int_{-1}^1 {\rm d}z\,(1 - z^2)^{(d-3)/2}\,, \tag{A.25}$$

where $d \equiv 3 - 2\epsilon$. The factorized integrals are, in general, ultraviolet divergent, and necessitate keeping track of $\epsilon \neq 0$. As always, a helpful strategy is to add and subtract a simple infrared finite regulator, such as $1/(k^2 + M^2)^\alpha$, where α is so chosen that the complicated expression becomes ultraviolet finite after the subtraction, and can be worked out at $\epsilon = 0$, while the ultraviolet divergent integral with the measure of eq. (A.25) is taken over the simple regulator. In the complicated but ultraviolet finite integral, it is useful to change integration variables from z to E_{p-k}, using

$$\int_{-1}^{+1}\frac{{\rm d}z}{E_{p-k}} = \int_{E_{p-k}^-}^{E_{p-k}^+}\frac{{\rm d}E_{p-k}}{pk}\,. \tag{A.26}$$

We should remark that in our particular example, S_4^0, the trick of adding and subtracting a regulator is superfluous, given that the divergent integral can be directly identified as a known case, but in the general case we have found it to be very helpful.

Now, because of the constraint $\delta(\omega - 2E_p)$ (for $\omega > 0$) in the factorized integrals, the integral over p can be carried out trivially. In fact, comparing eq. (A.11) with (B.3), which defines a corresponding 1-loop integral (denoted by $S_1(\omega)$ and given explicitly in eq. (B.4)), we arrive at

$$\begin{aligned} S_4^0(\omega)\big|_{\rm fz} &= S_1(\omega)\int_0^\infty \frac{{\rm d}k^0}{\pi}\,\mu^{2\epsilon}\int\frac{{\rm d}^d\mathbf{k}}{(2\pi)^d 2E_{p-k}}\rho(k^0,\mathbf{k})\Big\{ \\ &\Big[(\Delta_{++}^{-1}+\Delta_{-+}^{-1})(1+n_{\rm B0}-n_{\rm F2})-(\Delta_{--}^{-1}+\Delta_{+-}^{-1})(n_{\rm B0}+n_{\rm F2})\Big]\Big\}_{p=\sqrt{\omega^2-4M^2}/2}\,. \end{aligned} \tag{A.27}$$

Let us first inspect the vacuum ($T=0$) part hereof, i.e. the term without $n_{\rm B0}$ or $n_{\rm F2}$. Inserting the free gluon spectral function from eq. (A.2), the multiplier of $S_1(\omega)$ becomes

$$\mathcal{B}_0 \equiv \mu^{2\epsilon}\int\frac{{\rm d}^d\mathbf{k}}{(2\pi)^d}\frac{1}{4kE_{p-k}}\left[\frac{1}{k+E_p+E_{p-k}}+\frac{1}{k-E_p+E_{p-k}}\right]_{p=\sqrt{\omega^2-4M^2}/2}\,. \tag{A.28}$$

This can be compared with the integral

$$B_0(P^2;0,M^2) \equiv \mu^{2\epsilon}\int\frac{{\rm d}^DK}{(2\pi)^D}\frac{1}{K^2[(P-K)^2+M^2]} \tag{A.29}$$

$$= \mu^{2\epsilon}\int\frac{{\rm d}^d\mathbf{k}}{(2\pi)^d}\frac{1}{4kE_{p-k}}\left[\frac{1}{ip_0+k+E_{p-k}}+\frac{1}{-ip_0+k+E_{p-k}}\right], \tag{A.30}$$

where we denoted $K=(k_0,\mathbf{k})$ and carried out the integral over k_0. In other words, $\mathcal{B}_0 = B_0(P_E^2;0,M^2)$, where

$$P_E \equiv (-iE_p, p\,\hat{\mathbf{e}})|_{p=\sqrt{\omega^2-4M^2}/2}\;,\quad P_E^2=-M^2\,, \tag{A.31}$$

and $\hat{\mathbf{e}}$ is a unit vector; the value of this standard vacuum integral reads

$$B_0(-M^2;0,M^2)=\frac{1}{(4\pi)^2}\left[\frac{1}{\epsilon}+\ln\frac{\bar{\mu}^2}{M^2}+2+\mathcal{O}(\epsilon)\right]. \tag{A.32}$$

Combining this with eq. (B.4), the factorized vacuum part becomes

$$\begin{aligned} S_4^0(\omega)\big|_{\rm fz}^{\rm vac} &= S_1(\omega)B_0(-M^2;0,M^2) \\ &= \theta(\omega-2M)\frac{(\omega^2-4M^2)^{\frac{1}{2}}}{4\omega(4\pi)^3}\tanh\Big(\frac{\beta\omega}{4}\Big)\left[\frac{1}{\epsilon}+\ln\frac{\bar{\mu}^4}{M^2(\omega^2-4M^2)}+4+\mathcal{O}(\epsilon)\right]. \end{aligned} \tag{A.33}$$

For completeness, we have even kept exponentially small thermal terms in the coefficient of $1/\epsilon$, given that it is useful to crosscheck the exact cancellation of ultraviolet poles; after this check, we set $\tanh(\beta\omega/4)=1+\mathcal{O}(\exp(-\beta M))$, given that $\omega\geq 2M$.

Consider then the thermal part of eq. (A.27). Again, we omit exponentially small terms $\sim \exp(-\beta M)$, and use the free gluon spectral function. Because of the remaining factor $n_{\rm B0}$, the k-integral is exponentially convergent, and we can set $\epsilon = 0$. Employing eq. (A.26) the thermal part becomes

$$\begin{aligned} S_4^0(\omega)\big|_{\rm fz}^T &= \frac{S_1(\omega)}{(4\pi)^2}\int_0^\infty {\rm d}k\, k\, n_{\rm B}(k) \int_{-1}^{+1} \frac{{\rm d}z}{E_{p-k}} \times \\ &\times \left[\frac{1}{k+E_p+E_{p-k}} + \frac{1}{k-E_p+E_{p-k}} - \frac{1}{k-E_p-E_{p-k}} - \frac{1}{k+E_p-E_{p-k}}\right]_{p=\sqrt{\omega^2-4M^2}/2} \\ &= \frac{S_1(\omega)}{(4\pi)^2 p}\int_0^\infty {\rm d}k\, n_{\rm B}(k) \times \\ &\times \ln\left|\frac{(k+E_p+E^+_{p-k})(k-E_p+E^+_{p-k})(k-E_p-E^+_{p-k})(k+E_p-E^+_{p-k})}{(k+E_p+E^-_{p-k})(k-E_p+E^-_{p-k})(k-E_p-E^-_{p-k})(k+E_p-E^-_{p-k})}\right|_{p=\sqrt{\omega^2-4M^2}/2} . \end{aligned} \tag{A.34}$$

Making use of

$$(k+\sigma E_p)^2 - (E^\tau_{p-k})^2 = 2k[\sigma E_p - \tau\, p]\,, \quad \sigma,\tau = \pm\,, \tag{A.35}$$

it can be seen that the argument of the logarithm evaluates to unity. Hence, $S_4^0(\omega)\big|_{\rm fz}^T = 0$.

To summarize, combining eqs. (A.23), (A.24), (A.33), we get

$$S_4^0(\omega) = S_4^0(\omega)\big|_{\rm ps}^T + S_4^0(\omega)\big|_{\rm ps}^{\rm vac} + S_4^0(\omega)\big|_{\rm fz}^{\rm vac}\,. \tag{A.36}$$

The other master sum-integrals can be worked out in the same way, and the final results are listed in appendix B.

Appendix B. General results for all master sum-integrals

We collect in this appendix the results for all the master sum-integrals entering the computation, obtained with the methods explained in appendix A. In each case, we list the definition of the sum-integral; an intermediate result obtained after carrying our the Matsubara sums and taking the discontinuity; and the final result, obtained after restricting to the free gluon spectral function, omitting terms suppressed by $\exp(-\beta M)$ (except from the ultraviolet divergences), and carrying out the final spatial integrations. As before, the integration measure for the spatial integrations is defined as

$$\int_{\mathbf{p}} \equiv \mu^{2\epsilon} \int \frac{\mathrm{d}^{3-2\epsilon}\mathbf{p}}{(2\pi)^{3-2\epsilon}} \,, \tag{B.1}$$

and $\bar{\mu}^2 = 4\pi\mu^2 e^{-\gamma_{\mathrm{E}}}$ denotes the $\overline{\mathrm{MS}}$ scale parameter. To simplify the expressions somewhat, we also make use of the shorthands listed in eqs. (A.12), (A.13). The subscripts "ps" and "fz" denote "phase space" and "factorized" integrations, respectively, in the sense of sec. A.2.

B.1. S_1

The sum-integral S_1 is defined as

$$S_1(\omega) \equiv \mathrm{Disc}\left[\sum\!\!\!\!\!\!\int_{\{P\}} \frac{1}{\Delta(P)\Delta(P-Q)}\right]_{Q=(-i\omega,\mathbf{0})} . \tag{B.2}$$

Carrying out the Matsubara sum and taking the discontinuity leads to

$$S_1(\omega) = \int_{\mathbf{p}} \frac{\pi}{4E_p^2}\Big[1-2n_{\mathrm{F}}(E_p)\Big]\Big[\delta(\omega-2E_p)-\delta(\omega+2E_p)\Big] \,. \tag{B.3}$$

The remaining integral is trivial due to the δ-function and, restricting to $\omega > 0$, we arrive at

$$S_1(\omega) = \theta(\omega-2M)\frac{(\omega^2-4M^2)^{\frac{1}{2}}}{16\pi\omega}\tanh\Big(\frac{\beta\omega}{4}\Big)\left[1+\epsilon\left(\ln\frac{\bar{\mu}^2}{\omega^2-4M^2}+2\right)+\mathcal{O}(\epsilon^2)\right] . \tag{B.4}$$

B.2. S_2

The sum-integral S_2 is defined as

$$S_2(\omega) \equiv \mathrm{Disc}\left[\sum\!\!\!\!\!\!\int_{\{P\}} \frac{1}{\Delta^2(P)\Delta(P-Q)}\right]_{Q=(-i\omega,\mathbf{0})} . \tag{B.5}$$

It is easy to see that $S_2 = -\frac{1}{2}\,\mathrm{d}S_1/\mathrm{d}M^2$. Therefore, from eq. (B.4), we obtain

$$S_2(\omega) = \theta(\omega-2M)\frac{(\omega^2-4M^2)^{-\frac{1}{2}}}{16\pi\omega}\tanh\Big(\frac{\beta\omega}{4}\Big)\left[1+\epsilon\ln\frac{\bar{\mu}^2}{\omega^2-4M^2}+\mathcal{O}(\epsilon^2)\right] . \tag{B.6}$$

B.3. S_3

The sum-integral S_3 is defined as

$$S_3(\omega) \equiv \mathrm{Disc}\left[\int_{-\infty}^{\infty}\frac{\mathrm{d}k^0}{\pi}\,\mathop{\sum\!\!\!\!\!\!\int}_{K\{P\}}\frac{\rho(k^0,\mathbf{k})}{k^0-ik_n}\,\frac{1}{\Delta(P)\Delta(P-Q-K)}\right]_{Q=(-i\omega,\mathbf{0})}. \tag{B.7}$$

Performing the Matsubara sums, taking the discontinuity, and making use of the antisymmetry of $\rho(k^0,\mathbf{k})$ yields

$$\begin{aligned} S_3(\omega) \;=\; & \int_0^\infty\frac{\mathrm{d}k^0}{\pi}\int_{\mathbf{k},\mathbf{p}}\rho(k^0,\mathbf{k})\frac{\pi}{4E_pE_{p-k}}\Big\{ \\ & \Big[\delta(\omega-\Delta_{++})-\delta(\omega+\Delta_{++})\Big]\Big[(1+n_{\mathrm{B}0})(1-n_{\mathrm{F}1}-n_{\mathrm{F}2})+n_{\mathrm{F}1}n_{\mathrm{F}2}\Big] \\ & +\Big[\delta(\omega-\Delta_{--})-\delta(\omega+\Delta_{--})\Big]\Big[-n_{\mathrm{B}0}(1-n_{\mathrm{F}1}-n_{\mathrm{F}2})+n_{\mathrm{F}1}n_{\mathrm{F}2}\Big] \\ & +\Big[\delta(\omega-\Delta_{+-})-\delta(\omega+\Delta_{+-})\Big]\Big[n_{\mathrm{B}0}n_{\mathrm{F}1}-(1+n_{\mathrm{B}0})n_{\mathrm{F}2}+n_{\mathrm{F}1}n_{\mathrm{F}2}\Big] \\ & +\Big[\delta(\omega-\Delta_{-+})-\delta(\omega+\Delta_{-+})\Big]\Big[n_{\mathrm{B}0}n_{\mathrm{F}2}-(1+n_{\mathrm{B}0})n_{\mathrm{F}1}+n_{\mathrm{F}1}n_{\mathrm{F}2}\Big]\Big\}\,. \end{aligned} \tag{B.8}$$

Inserting the free gluon spectral function, and omitting exponentially small terms, yields

$$\begin{aligned} S_3(\omega) \;=\; & \frac{1}{(4\pi)^3}\Big\{\theta(\omega-2M)\Big[\frac{(\omega^2-4M^2)^{\frac{1}{2}}\,(\omega^2+2M^2)}{8\omega}+\frac{M^2(M^2-\omega^2)}{\omega^2}\,\mathrm{acosh}\Big(\frac{\omega}{2M}\Big)\Big] \\ & +\int_0^\infty\mathrm{d}k\,k\,n_{\mathrm{B}}(k)\Big[\theta(\omega)\,\theta\Big(k-\frac{4M^2-\omega^2}{2\omega}\Big)\sqrt{1-\frac{4M^2}{\omega(\omega+2k)}} \\ & +\theta(\omega-2M)\,\theta\Big(\frac{\omega^2-4M^2}{2\omega}-k\Big)\sqrt{1-\frac{4M^2}{\omega(\omega-2k)}}\;\Big]\Big\}+\mathcal{O}(e^{-\beta M})\,. \end{aligned} \tag{B.9}$$

B.4. S_4^0

The sum-integral S_4^0 is defined in eq. (A.5); its value after the Matsubara sums is given in eq. (A.11); the result after the phase space integrals is the sum of eqs. (A.23), (A.24), (A.33).

B.5. S_4^1

The sum-integral S_4^1 is defined as

$$S_4^1(\omega) \equiv \mathrm{Disc}\left[\int_{-\infty}^{\infty}\frac{\mathrm{d}k^0}{\pi}\,\mathop{\sum\!\!\!\!\!\!\int}_{K\{P\}}\frac{\rho(k^0,\mathbf{k})}{k^0-ik_n}\,\frac{Q\cdot K}{\Delta(P)\Delta(P-Q)\Delta(P-K)}\right]_{Q=(-i\omega,\mathbf{0})}. \tag{B.10}$$

Performing the Matsubara sums, taking the discontinuity, and making use of the antisymmetry of $\rho(k^0,\mathbf{k})$ yields

$$
\begin{aligned}
S_4^1(\omega) \;=\; & \int_0^\infty \frac{\mathrm{d}k^0}{\pi}\int_{\mathbf{k},\mathbf{p}} \rho(k^0,\mathbf{k})\frac{\pi k^0\omega}{4E_pE_{p-k}}\Big\{ \\
& \frac{1}{2E_p}\Big[\delta(\omega-2E_p)+\delta(\omega+2E_p)\Big](1-2n_{\mathrm{F1}})\times \\
& \times\Big[(\Delta^{-1}_{++}-\Delta^{-1}_{-+})(1+n_{\mathrm{B0}}-n_{\mathrm{F2}})+(\Delta^{-1}_{--}-\Delta^{-1}_{+-})(n_{\mathrm{B0}}+n_{\mathrm{F2}})\Big] \\
& +\Big[\delta(\omega-\Delta_{++})+\delta(\omega+\Delta_{++})\Big]\Delta^{-1}_{++}\Delta^{-1}_{-+}\Big[(1+n_{\mathrm{B0}})(1-n_{\mathrm{F1}}-n_{\mathrm{F2}})+n_{\mathrm{F1}}n_{\mathrm{F2}}\Big] \\
& +\Big[\delta(\omega-\Delta_{--})+\delta(\omega+\Delta_{--})\Big]\Delta^{-1}_{--}\Delta^{-1}_{+-}\Big[-n_{\mathrm{B0}}(1-n_{\mathrm{F1}}-n_{\mathrm{F2}})+n_{\mathrm{F1}}n_{\mathrm{F2}}\Big] \\
& +\Big[\delta(\omega-\Delta_{+-})+\delta(\omega+\Delta_{+-})\Big]\Delta^{-1}_{--}\Delta^{-1}_{+-}\Big[n_{\mathrm{B0}}n_{\mathrm{F1}}-(1+n_{\mathrm{B0}})n_{\mathrm{F2}}+n_{\mathrm{F1}}n_{\mathrm{F2}}\Big] \\
& +\Big[\delta(\omega-\Delta_{-+})+\delta(\omega+\Delta_{-+})\Big]\Delta^{-1}_{++}\Delta^{-1}_{-+}\Big[n_{\mathrm{B0}}n_{\mathrm{F2}}-(1+n_{\mathrm{B0}})n_{\mathrm{F1}}+n_{\mathrm{F1}}n_{\mathrm{F2}}\Big]\Big\}\,.
\end{aligned}
\tag{B.11}
$$

Inserting the free gluon spectral function, the ultraviolet divergent factorized vacuum part reads

$$
S_4^1(\omega)\big|^{\mathrm{vac}}_{\mathrm{fz}} \;=\; -\theta(\omega-2M)\frac{\omega(\omega^2-4M^2)^{\frac{1}{2}}}{16(4\pi)^3}\tanh\Big(\frac{\beta\omega}{4}\Big)\Big[\frac{1}{\epsilon}+\ln\frac{\bar{\mu}^4}{M^2(\omega^2-4M^2)}+3+\mathcal{O}(\epsilon)\Big]\,,
\tag{B.12}
$$

where in the coefficient of the divergence we have accounted even for exponentially small terms. The vacuum part from the phase space integrals reads

$$
S_4^1(\omega)\big|^{\mathrm{vac}}_{\mathrm{ps}} \;=\; \frac{\theta(\omega-2M)}{(4\pi)^3}\Big[\frac{3(\omega^2-4M^2)^{\frac{1}{2}}(2M^2-\omega^2)}{32\omega}+\frac{\omega^4-4\omega^2M^2+6M^4}{8\omega^2}\,\mathrm{acosh}\Big(\frac{\omega}{2M}\Big)\Big]\,,
\tag{B.13}
$$

while the thermal parts amount to

$$
S_4^1(\omega)\big|^{T}_{\mathrm{fz}} \;=\; \frac{1}{(4\pi)^3}\Big\{\int_0^\infty \mathrm{d}k\,k\,n_{\mathrm{B}}(k)\theta(\omega-2M)\Big[-2\,\mathrm{acosh}\Big(\frac{\omega}{2M}\Big)\Big]\Big\}+\mathcal{O}(e^{-\beta M})\,,
\tag{B.14}
$$

$$
\begin{aligned}
S_4^1(\omega)\big|^{T}_{\mathrm{ps}} \;=\; & \frac{1}{(4\pi)^3}\Big\{\int_0^\infty \mathrm{d}k\,k\,n_{\mathrm{B}}(k)\Big[\theta(\omega)\,\theta\Big(k-\frac{4M^2-\omega^2}{2\omega}\Big)\,\mathrm{acosh}\sqrt{\frac{\omega(\omega+2k)}{4M^2}} \\
& +\theta(\omega-2M)\,\theta\Big(\frac{\omega^2-4M^2}{2\omega}-k\Big)\,\mathrm{acosh}\sqrt{\frac{\omega(\omega-2k)}{4M^2}}\Big]\Big\}+\mathcal{O}(e^{-\beta M})\,.
\end{aligned}
\tag{B.15}
$$

B.6. S_4^2

The sum-integral S_4^2 is defined as

$$S_4^2(\omega) \equiv \mathrm{Disc}\left[\sum\!\!\!\!\!\!\int_{K\{P\}} \frac{1}{K^2}\frac{K^2}{\Delta(P)\Delta(P-Q)\Delta(P-K)}\right]_{Q=(-i\omega,\mathbf{0})} . \tag{B.16}$$

Because of the ultraviolet divergent factor in the numerator, the use of the spectral representation requires care in this case, and we rather proceed directly with the sum, having gone over into free gluons to start with. Carrying out the shift $K \to P-K$, the summation factorizes,

$$S_4^2(\omega) = \mathrm{Disc}\left[\sum\!\!\!\!\!\!\int_{\{P\}} \frac{1}{\Delta(P)\Delta(P-Q)}\right]_{Q=(-i\omega,\mathbf{0})} \times \sum\!\!\!\!\!\!\int_{\{K\}} \frac{1}{\Delta(K)} = S_1(\omega)\, I_0(M^2) , \tag{B.17}$$

where $S_1(\omega)$ is given in eq. (B.4), while I_0 is a basic tadpole integral generalized to finite temperature. In fact, the finite temperature effects in I_0 are exponentially small and can be omitted:

$$I_0(M^2) \;=\; \int_{\mathbf{k}} \frac{1}{2k}\Big[1-2n_{\mathrm{F}}(E_k)\Big] = -\frac{M^2}{(4\pi)^2}\left[\frac{1}{\epsilon}+\ln\frac{\bar{\mu}^2}{M^2}+1\right]+\mathcal{O}(\epsilon,e^{-\beta M}) . \tag{B.18}$$

Keeping exponentially small terms in the coefficient of the divergence, though, we arrive at

$$S_4^2(\omega) = -\theta(\omega-2M)\frac{(\omega^2-4M^2)^{\frac{1}{2}}\,M^2}{4\omega(4\pi)^3}\tanh\Big(\frac{\beta\omega}{4}\Big)\left[\frac{1}{\epsilon}+\ln\frac{\bar{\mu}^4}{M^2(\omega^2-4M^2)}+3+\mathcal{O}(\epsilon,e^{-\beta M})\right] . \tag{B.19}$$

B.7. S_5^0

The sum-integral S_5^0 is defined as

$$S_5^0(\omega) \equiv \mathrm{Disc}\left[\int_{-\infty}^{\infty}\frac{\mathrm{d}k^0}{\pi}\sum\!\!\!\!\!\!\int_{K\{P\}} \frac{\rho(k^0,\mathbf{k})}{k^0-ik_n}\frac{1}{\Delta^2(P)\Delta(P-Q)\Delta(P-K)}\right]_{Q=(-i\omega,\mathbf{0})} . \tag{B.20}$$

Performing the Matsubara sums, taking the discontinuity, and making use of the antisymmetry of $\rho(k^0,\mathbf{k})$ yields

$$
\begin{aligned}
S_5^0(\omega) \;=\; & \int_0^\infty \frac{\mathrm{d}k^0}{\pi}\int_{\mathbf{k},\mathbf{p}} \rho(k^0,\mathbf{k})\frac{\pi}{8E_p^2E_{p-k}}\Big\{ \\
& \frac{1}{2E_p}\Big[\delta(\omega-2E_p)-\delta(\omega+2E_p)\Big](1-2n_{\mathrm{F1}})\times \\
& \times\Big[(\Delta_{++}^{-1}+\Delta_{-+}^{-1})(\Delta_{++}^{-1}-\Delta_{-+}^{-1}+E_p^{-1})(1+n_{\mathrm{B0}}-n_{\mathrm{F2}}) \\
& \quad +(\Delta_{--}^{-1}+\Delta_{+-}^{-1})(\Delta_{--}^{-1}-\Delta_{+-}^{-1}-E_p^{-1})(n_{\mathrm{B0}}+n_{\mathrm{F2}})\Big] \\
- \;& \frac{\beta}{2E_p}\Big[\delta(\omega-2E_p)-\delta(\omega+2E_p)\Big](1-n_{\mathrm{F1}})n_{\mathrm{F1}}\times \\
& \times\Big[(\Delta_{++}^{-1}+\Delta_{-+}^{-1})(1+n_{\mathrm{B0}}-n_{\mathrm{F2}})-(\Delta_{--}^{-1}+\Delta_{+-}^{-1})(n_{\mathrm{B0}}+n_{\mathrm{F2}})\Big] \\
+ \;& \frac{1}{2E_p}\Big[\delta'(\omega-2E_p)+\delta'(\omega+2E_p)\Big](1-2n_{\mathrm{F1}})\times \\
& \times\Big[(\Delta_{++}^{-1}+\Delta_{-+}^{-1})(1+n_{\mathrm{B0}}-n_{\mathrm{F2}})-(\Delta_{--}^{-1}+\Delta_{+-}^{-1})(n_{\mathrm{B0}}+n_{\mathrm{F2}})\Big] \\
+ \;& \Big[\delta(\omega-\Delta_{++})-\delta(\omega+\Delta_{++})\Big]\Delta_{++}^{-1}\Delta_{-+}^{-1}(\Delta_{-+}^{-1}-\Delta_{++}^{-1})\times \\
& \qquad\times\Big[(1+n_{\mathrm{B0}})(1-n_{\mathrm{F1}}-n_{\mathrm{F2}})+n_{\mathrm{F1}}n_{\mathrm{F2}}\Big] \\
& +\Big[\delta(\omega-\Delta_{--})-\delta(\omega+\Delta_{--})\Big]\Delta_{--}^{-1}\Delta_{+-}^{-1}(\Delta_{--}^{-1}-\Delta_{+-}^{-1})\times \\
& \qquad\times\Big[-n_{\mathrm{B0}}(1-n_{\mathrm{F1}}-n_{\mathrm{F2}})+n_{\mathrm{F1}}n_{\mathrm{F2}}\Big] \\
& +\Big[\delta(\omega-\Delta_{+-})-\delta(\omega+\Delta_{+-})\Big]\Delta_{--}^{-1}\Delta_{+-}^{-1}(\Delta_{--}^{-1}-\Delta_{+-}^{-1})\times \\
& \qquad\times\Big[n_{\mathrm{B0}}n_{\mathrm{F1}}-(1+n_{\mathrm{B0}})n_{\mathrm{F2}}+n_{\mathrm{F1}}n_{\mathrm{F2}}\Big] \\
& +\Big[\delta(\omega-\Delta_{-+})-\delta(\omega+\Delta_{-+})\Big]\Delta_{++}^{-1}\Delta_{-+}^{-1}(\Delta_{-+}^{-1}-\Delta_{++}^{-1})\times \\
& \qquad\times\Big[n_{\mathrm{B0}}n_{\mathrm{F2}}-(1+n_{\mathrm{B0}})n_{\mathrm{F1}}+n_{\mathrm{F1}}n_{\mathrm{F2}}\Big]\Big\}\,.
\end{aligned}
\tag{B.21}
$$

In the factorized part, it is useful to carry out a partial integration in order to remove the structure $\delta'(\omega-2E_p)+\delta'(\omega+2E_p)$:

$$
\begin{aligned}
& \int\frac{\mathrm{d}^d\mathbf{p}}{(2\pi)^d}\delta'(\omega-2E_p)g(p,E_p,E_{p-k}) \\
& \quad= \int\frac{\mathrm{d}^d\mathbf{p}}{(2\pi)^d}\delta(\omega-2E_p)\Big\{\frac{(d-2)E_pg}{2p^2}+\frac{E_p}{2p}\frac{\partial g}{\partial p}+\frac{1}{2E_p}\frac{\partial(E_pg)}{\partial E_p}+\frac{(p+kz)E_p}{2pE_{p-k}}\frac{\partial g}{\partial E_{p-k}}\Big\}\,.
\end{aligned}
\tag{B.22}
$$

The subsequent steps proceed as described in appendix A.

In contrast to S_4^0, S_4^1, however, it is not possible to give separate closed expressions for the factorized and phase space vacuum parts of S_5^0, because the integrals are logarithmi-

cally divergent at the lower limit of the k-integration (in the thermal case, they are linearly divergent). Yet the sum is finite, and inserting the free gluon spectral function, we get

$$S_5^0(\omega)\Big|^{\rm vac} = \frac{\theta(\omega-2M)}{4\omega(4\pi)^3(\omega^2-4M^2)^{\frac{1}{2}}}\biggl\{\tanh\Bigl(\frac{\beta\omega}{4}\Bigr)\biggl[\frac{1}{\epsilon}+\ln\frac{\bar{\mu}^4}{M^2(\omega^2-4M^2)}+2\biggr] \tag{B.23}$$
$$+\,\frac{\omega^2-4M^2}{M^2}\ln\frac{\omega(\omega^2-4M^2)}{M^3}+\frac{(\omega^2-4M^2)^{\frac{1}{2}}\,(4M^2-3\omega^2)}{\omega M^2}\,\mathrm{acosh}\biggl(\frac{\omega}{2M}\biggr)\biggr\}+\mathcal{O}(\epsilon)\;,$$

where in the coefficient of the divergence we have accounted even for exponentially small thermal corrections. For the thermal part proper we obtain

$$S_5^0(\omega)\Big|^{T} = \frac{1}{4\omega^2M^2(4\pi)^3}\int_0^\infty\mathrm{d}k\,\frac{n_{\rm B}(k)}{k}\biggl[\tag{B.24}$$
$$\theta(\omega)\,\theta\Bigl(k-\frac{4M^2-\omega^2}{2\omega}\Bigr)\sqrt{\omega(\omega+2k)}\sqrt{\omega(\omega+2k)-4M^2}$$
$$+\theta(\omega-2M)\,\theta\Bigl(\frac{\omega^2-4M^2}{2\omega}-k\Bigr)\sqrt{\omega(\omega-2k)}\sqrt{\omega(\omega-2k)-4M^2}$$
$$-\theta(\omega-2M)\times 2\omega\sqrt{\omega^2-4M^2}\,\biggr]+\mathcal{O}(e^{-\beta M})\;.$$

The last line, which originates from the factorized integrals, subtracts the values of the first two lines at $k=0$ (for $\omega>2M$), rendering the integral infrared finite.

B.8. $\hat{S}_5^0$

The sum-integral $\hat{S}_5^0$ is defined as

$$\hat{S}_5^0(\omega)\equiv\mathrm{Disc}\biggl[\int_{-\infty}^{\infty}\frac{\mathrm{d}k^0}{\pi}\sum\!\!\!\!\!\!\int_{K\{P\}}\frac{\rho(k^0,\mathbf{k})}{k^0-ik_n}\frac{\mathbf{p}^2-(\mathbf{p}\cdot\hat{\mathbf{k}})^2}{\Delta^2(P)\Delta(P-Q)\Delta(P-K)}\biggr]_{Q=(-i\omega,\mathbf{0})}\;. \tag{B.25}$$

Carrying out the Matsubara sums proceeds precisely like for S_5^0, and leads to an expression like eq. (B.21); it is also again useful to carry out the partial integration in eq. (B.22). The subsequent steps lead to the vacuum part

$$\hat{S}_5^0(\omega)\Big|^{\rm vac} = \frac{\theta(\omega-2M)(\omega^2-4M^2)^{\frac{1}{2}}}{8\omega(4\pi)^3}\biggl\{\tanh\Bigl(\frac{\beta\omega}{4}\Bigr)\biggl[\frac{1}{\epsilon}+\ln\frac{\bar{\mu}^4}{M^2(\omega^2-4M^2)}+1\biggr]$$
$$-\,4\ln\frac{\omega(\omega^2-4M^2)}{M^3}+\frac{2(7\omega^2-8M^2)}{\omega(\omega^2-4M^2)^{\frac{1}{2}}}\,\mathrm{acosh}\biggl(\frac{\omega}{2M}\biggr)$$
$$+\,\frac{2\omega}{(\omega^2-4M^2)^{\frac{1}{2}}}\alpha\biggl(\frac{\sqrt{\omega^2-4M^2}}{\omega}\biggr)\biggr\}+\mathcal{O}(\epsilon)\;. \tag{B.26}$$

Here the function

$$\alpha(v) \equiv \int_0^\infty \frac{\mathrm{d}x}{x}\bigg[\theta(v^2-x)(1-x)\ln\frac{\sqrt{1-x}+\sqrt{v^2-x}}{\sqrt{1-x}-\sqrt{v^2-x}} + \ln\frac{(1+x+\sqrt{1+2vx+x^2})(-1+x+\sqrt{1-2vx+x^2})}{(1+x+\sqrt{1-2vx+x^2})(-1+x+\sqrt{1+2vx+x^2})}\bigg] , \quad \text{(B.27)}$$

where the integration variable x is related to k through $k = x\omega/2$, is finite, but we have not bothered to work out its analytic expression, given that it does not appear in our final result. The thermal part reads

$$\begin{aligned}\hat{S}_5^0(\omega)\Big|^T = \frac{1}{2\omega^2(4\pi)^3}\int_0^\infty \mathrm{d}k\,\frac{n_{\mathrm{B}}(k)}{k}\bigg\{ & \qquad \text{(B.28)}\\ & \theta(\omega)\,\theta\bigg(k-\frac{4M^2-\omega^2}{2\omega}\bigg)\times \\ & \times\bigg[-\sqrt{\omega(\omega+2k)}\sqrt{\omega(\omega+2k)-4M^2}+\omega(\omega+2k)\,\mathrm{acosh}\sqrt{\frac{\omega(\omega+2k)}{4M^2}}\bigg] \\ & +\theta(\omega-2M)\,\theta\bigg(\frac{\omega^2-4M^2}{2\omega}-k\bigg)\times \\ & \times\bigg[-\sqrt{\omega(\omega-2k)}\sqrt{\omega(\omega-2k)-4M^2}+\omega(\omega-2k)\,\mathrm{acosh}\sqrt{\frac{\omega(\omega-2k)}{4M^2}}\bigg] \\ & +\theta(\omega-2M)\times\bigg[2\omega\sqrt{\omega^2-4M^2}-2\omega^2\,\mathrm{acosh}\bigg(\frac{\omega}{2M}\bigg)\bigg]\bigg\}+\mathcal{O}(e^{-\beta M}) .\end{aligned}$$

The last line, which originates from the factorized integrals, subtracts the values of the first two lines at $k = 0$ (for $\omega > 2M$), rendering the integral infrared finite.

B.9. S_5^2

The sum-integral S_5^2 is defined as

$$S_5^2(\omega) \equiv \mathrm{Disc}\bigg[\sum\!\!\!\!\!\!\int_{K\{P\}} \frac{1}{K^2}\frac{K^2}{\Delta^2(P)\Delta(P-Q)\Delta(P-K)}\bigg]_{Q=(-i\omega,\mathbf{0})} . \quad \text{(B.29)}$$

Because of the ultraviolet divergent factor in the numerator, the use of the spectral representation requires care in this case, and we rather proceed directly with the sum, as in the case of S_4^2. Carrying out the shift $K \to P - K$, the summation factorizes,

$$S_5^2(\omega) = \mathrm{Disc}\bigg[\sum\!\!\!\!\!\!\int_{\{P\}} \frac{1}{\Delta^2(P)\Delta(P-Q)}\bigg]_{Q=(-i\omega,\mathbf{0})} \times \sum\!\!\!\!\!\!\int_{\{K\}} \frac{1}{\Delta(K)} = S_2(\omega)\,I_0(M^2) , \quad \text{(B.30)}$$

where $S_2(\omega)$ is given in eq. (B.6), while I_0 is given in eq. (B.18). Keeping exponentially small terms in the coefficient of the divergence, we arrive at

$$S_5^2(\omega) = -\frac{\theta(\omega-2M)M^2}{4\omega(\omega^2-4M^2)^{\frac{1}{2}}(4\pi)^3}\tanh\Big(\frac{\beta\omega}{4}\Big)\left[\frac{1}{\epsilon}+\ln\frac{\bar{\mu}^4}{M^2(\omega^2-4M^2)}+1+\mathcal{O}(\epsilon,e^{-\beta M})\right]. \tag{B.31}$$

B.10. S_6^0

The sum-integral S_6^0 is defined as

$$S_6^0(\omega) \equiv \mathrm{Disc}\left[\int_{-\infty}^{\infty}\frac{\mathrm{d}k^0}{\pi}\sum\!\!\!\!\!\!\int_{K\{P\}}\frac{\rho(k^0,\mathbf{k})}{k^0-ik_n}\frac{1}{\Delta(P)\Delta(P-Q)\Delta(P-K)\Delta(P-Q-K)}\right]_{Q=(-i\omega,\mathbf{0})}. \tag{B.32}$$

Performing the Matsubara sums, taking the discontinuity, and making use of the antisymmetry of $\rho(k^0,\mathbf{k})$ yields

$$\begin{aligned}
S_6^0(\omega) \;=\; & \int_0^\infty\frac{\mathrm{d}k^0}{\pi}\int_{\mathbf{k},\mathbf{p}}\rho(k^0,\mathbf{k})\frac{\pi}{2E_pE_{p-k}}\Bigg\{ \\
& \frac{1}{8E_p^2}\Big[\delta(\omega-2E_p)-\delta(\omega+2E_p)\Big](1-2n_{\mathrm{F}1})\times \\
& \times\Bigg[\left(\frac{\Delta_{--}^{-1}}{E_p+E_{p-k}}+\frac{\Delta_{+-}^{-1}}{E_p-E_{p-k}}\right)(n_{\mathrm{B}0}+n_{\mathrm{F}2}) \\
& -\left(\frac{\Delta_{++}^{-1}}{E_p+E_{p-k}}+\frac{\Delta_{-+}^{-1}}{E_p-E_{p-k}}\right)(1+n_{\mathrm{B}0}-n_{\mathrm{F}2})\Bigg] \\
+\quad & \frac{1}{8E_{p-k}^2}\Big[\delta(\omega-2E_{p-k})-\delta(\omega+2E_{p-k})\Big](1-2n_{\mathrm{F}2})\times \\
& \times\Bigg[\left(\frac{\Delta_{--}^{-1}}{E_{p-k}+E_p}+\frac{\Delta_{-+}^{-1}}{E_{p-k}-E_p}\right)(n_{\mathrm{B}0}+n_{\mathrm{F}1}) \\
& -\left(\frac{\Delta_{++}^{-1}}{E_{p-k}+E_p}+\frac{\Delta_{+-}^{-1}}{E_{p-k}-E_p}\right)(1+n_{\mathrm{B}0}-n_{\mathrm{F}1})\Bigg] \\
+\quad & \Big[\delta(\omega-\Delta_{++})-\delta(\omega+\Delta_{++})\Big]\Delta_{++}^{-2}\Delta_{+-}^{-1}\Delta_{-+}^{-1}\Big[(1+n_{\mathrm{B}0})(1-n_{\mathrm{F}1}-n_{\mathrm{F}2})+n_{\mathrm{F}1}n_{\mathrm{F}2}\Big] \\
& +\Big[\delta(\omega-\Delta_{--})-\delta(\omega+\Delta_{--})\Big]\Delta_{--}^{-2}\Delta_{+-}^{-1}\Delta_{-+}^{-1}\Big[-n_{\mathrm{B}0}(1-n_{\mathrm{F}1}-n_{\mathrm{F}2})+n_{\mathrm{F}1}n_{\mathrm{F}2}\Big] \\
& +\Big[\delta(\omega-\Delta_{+-})-\delta(\omega+\Delta_{+-})\Big]\Delta_{+-}^{-2}\Delta_{++}^{-1}\Delta_{--}^{-1}\Big[n_{\mathrm{B}0}n_{\mathrm{F}1}-(1+n_{\mathrm{B}0})n_{\mathrm{F}2}+n_{\mathrm{F}1}n_{\mathrm{F}2}\Big] \\
& +\Big[\delta(\omega-\Delta_{-+})-\delta(\omega+\Delta_{-+})\Big]\Delta_{-+}^{-2}\Delta_{++}^{-1}\Delta_{--}^{-1}\Big[n_{\mathrm{B}0}n_{\mathrm{F}2}-(1+n_{\mathrm{B}0})n_{\mathrm{F}1}+n_{\mathrm{F}1}n_{\mathrm{F}2}\Big]\Bigg\}.
\end{aligned} \tag{B.33}$$

In the factorized part, a change of integration variables $\mathbf{p}\to\mathbf{k}-\mathbf{p}$ allows trivially to change the structure with $\delta(\omega-2E_{p-k})-\delta(\omega+2E_{p-k})$ into the familiar one with $\delta(\omega-2E_p)-$

$\delta(\omega + 2E_p)$. (The only complication is that then the difference $1/(E_p - E_{p-k})$ needs to be interpreted as a principal value.) The subsequent steps proceed as described in appendix A.

Like with S_5^0, it is again not possible to give separate closed expressions for the factorized and phase space vacuum parts of S_6^0, because the integrals are logarithmically divergent at the lower limit of the k-integration (in the thermal case, they are linearly divergent). The sum is infrared finite, however, and inserting the free gluon spectral function, yields [3]

$$S_6^0(\omega)\Big|^{\rm vac} \;=\; \frac{\theta(\omega-2M)}{\omega^2(4\pi)^3} L_2\Big(\frac{\omega-\sqrt{\omega^2-4M^2}}{\omega+\sqrt{\omega^2-4M^2}}\Big) + \mathcal{O}(\epsilon)\;, \tag{B.34}$$

where the function L_2 is defined in eq. (4.6). For the thermal parts we obtain, omitting exponentially small terms,

$$\begin{aligned} S_6^0(\omega)\Big|^{T} \;=\; \frac{2}{\omega^2(4\pi)^3}\int_0^\infty {\rm d}k\,\frac{n_{\rm B}(k)}{k}\Big[& \\ & \theta(\omega)\,\theta\Big(k-\frac{4M^2-\omega^2}{2\omega}\Big)\,{\rm acosh}\sqrt{\frac{\omega(\omega+2k)}{4M^2}} \\ & +\theta(\omega-2M)\,\theta\Big(\frac{\omega^2-4M^2}{2\omega}-k\Big)\,{\rm acosh}\sqrt{\frac{\omega(\omega-2k)}{4M^2}} \\ & -\theta(\omega-2M)\times 2\,{\rm acosh}\Big(\frac{\omega}{2M}\Big)\Big] + \mathcal{O}(e^{-\beta M})\;. \end{aligned} \tag{B.35}$$

The last line, which originates from the factorized integrals, subtracts the values of the first two lines at $k=0$ (for $\omega > 2M$), rendering the integral infrared finite.

B.11. $\hat{S}_6^0$

The sum-integral $\hat{S}_6^0$ is defined as

$$\hat{S}_6^0(\omega) \equiv {\rm Disc}\,\Big[\int_{-\infty}^{\infty}\frac{{\rm d}k^0}{\pi}\,\mathop{\sum\!\!\!\!\!\!\int\!\!\!\!\!\!\int}_{K\{P\}}\frac{\rho(k^0,\mathbf{k})}{k^0-ik_n}\,\frac{\mathbf{p}^2-(\mathbf{p}\cdot\hat{\mathbf{k}})^2}{\Delta(P)\Delta(P-Q)\Delta(P-K)\Delta(P-Q-K)}\Big]_{Q=(-i\omega,\mathbf{0})}\;. \tag{B.36}$$

Carrying out the Matsubara sums proceeds precisely like for S_6^0, and leads to an expression like eq. (B.33). The subsequent steps lead to the vacuum part

$$\hat{S}_6^0(\omega)\Big|^{\rm vac} \;=\; \frac{\theta(\omega-2M)}{\omega^2(4\pi)^3}\Big[-M^2 L_2\Big(\frac{\omega-\sqrt{\omega^2-4M^2}}{\omega+\sqrt{\omega^2-4M^2}}\Big) + \frac{\omega^2}{2}\beta\Big(\frac{\sqrt{\omega^2-4M^2}}{\omega}\Big)\Big] + \mathcal{O}(\epsilon)\;. \tag{B.37}$$

Here the function

$$\begin{aligned} \beta(v) \;\equiv\; & \int_0^\infty\frac{{\rm d}x}{x}\Big[\theta(v^2-x)\sqrt{1-x}\sqrt{v^2-x} - v + \frac{3}{4}\Big(\sqrt{1+2vx+x^2}-\sqrt{1-2vx+x^2}\Big) \\ & + \frac{x^2-4}{8}\ln\Big|\frac{(1+\sqrt{1+2vx+x^2})(-1+\sqrt{1-2vx+x^2})}{(1+\sqrt{1-2vx+x^2})(-1+\sqrt{1+2vx+x^2})}\Big|\Big] \end{aligned} \tag{B.38}$$

where the integration variable x is related to k through $k = x\omega/2$, is finite, but we have not bothered to work out its analytic expression, given that it does not appear in our final result. The thermal part reads

$$\begin{aligned}\hat{S}_6^0(\omega)\Big|^T \;=\; & \frac{1}{2\omega^2(4\pi)^3}\int_0^\infty \mathrm{d}k\,\frac{n_{\rm B}(k)}{k}\Bigg\{ \\ & \theta(\omega)\,\theta\!\left(k-\frac{4M^2-\omega^2}{2\omega}\right)\times \\ & \times\left[\sqrt{\omega(\omega+2k)}\sqrt{\omega(\omega+2k)-4M^2}-4M^2\,\mathrm{acosh}\sqrt{\frac{\omega(\omega+2k)}{4M^2}}\right] \\ & +\theta(\omega-2M)\,\theta\!\left(\frac{\omega^2-4M^2}{2\omega}-k\right)\times \\ & \times\left[\sqrt{\omega(\omega-2k)}\sqrt{\omega(\omega-2k)-4M^2}-4M^2\,\mathrm{acosh}\sqrt{\frac{\omega(\omega-2k)}{4M^2}}\right] \\ & +\theta(\omega-2M)\times\left[-2\omega\sqrt{\omega^2-4M^2}+8M^2\,\mathrm{acosh}\left(\frac{\omega}{2M}\right)\right]\Bigg\}+\mathcal{O}(e^{-\beta M})\;.\end{aligned} \tag{B.39}$$

The last line, which originates from the factorized integrals, subtracts the values of the first two lines at $k = 0$ (for $\omega > 2M$), rendering the integral infrared finite.

B.12. S_6^2

The sum-integral S_6^2 is defined as

$$S_6^2(\omega) \equiv \mathrm{Disc}\left[\sum\!\!\!\!\!\!\int_{K\{P\}} \frac{1}{K^2}\frac{K^2}{\Delta(P)\Delta(P-Q)\Delta(P-K)\Delta(P-Q-K)}\right]_{Q=(-i\omega,\mathbf{0})}. \tag{B.40}$$

Like with S_4^2 and S_5^2, we proceed directly with free gluons rather than using the spectral representation. Carrying out the shift $K \to P - K$, the summation factorizes,

$$\begin{aligned} S_6^2(\omega) \;&=\; \mathrm{Disc}\left\{\left[\sum\!\!\!\!\!\!\int_{\{P\}}\frac{1}{\Delta(P)\Delta(P-Q)}\right]_{Q=(-i\omega,\mathbf{0})}\times\left[\sum\!\!\!\!\!\!\int_{\{K\}}\frac{1}{\Delta(K)\Delta(K-Q)}\right]_{Q=(-i\omega,\mathbf{0})}\right\} \\ &=\; 2\,\mathrm{Re}\left[\sum\!\!\!\!\!\!\int_{\{P\}}\frac{1}{\Delta(P)\Delta(P-Q)}\right]_{Q=(-i\omega,\mathbf{0})}\times\mathrm{Disc}\left[\sum\!\!\!\!\!\!\int_{\{K\}}\frac{1}{\Delta(K)\Delta(K-Q)}\right]_{Q=(-i\omega,\mathbf{0})}, \end{aligned} \tag{B.41}$$

where Re[...] denotes the regular (non-discontinuous) part, while the discontinuous part can be identified with the function $S_1(\omega)$, given in eq. (B.4). The Matsubara sum in the regular part can be carried out as before; the only difference with respect to the procedure in appendix A is that taking the regular part after the substitution $\omega_n \to -i\omega$ yields a principle value rather

than a delta-function:

$$\begin{aligned}
&\mathrm{Re}\Big[\sum\!\!\!\!\!\!\int_{\{P\}} \frac{1}{\Delta(P)\Delta(P-Q)}\Big]_{Q=(-i\omega,\mathbf{0})} \\
&\quad = \int_{\mathbf{p}} \frac{1}{4E_p^2}\bigg[P\bigg(\frac{1}{\omega+2E_p}\bigg) - P\bigg(\frac{1}{\omega-2E_p}\bigg)\bigg]\Big[1-2n_{\mathrm{F}}(E_p)\Big] \,. \qquad \text{(B.42)}
\end{aligned}$$

It is seen that the finite-temperature effects continue to be exponentially suppressed. The zero-temperature part, on the other hand, equals the real part of the general function B_0, another special case of which was met in eq. (A.29):

$$\begin{aligned}
&\mathrm{Re}\bigg[\mu^{2\epsilon}\int\frac{\mathrm{d}^D P}{(2\pi)^D}\frac{1}{(P^2+M^2)[(P-Q)^2+M^2]}\bigg]_{Q=(-i\omega,\mathbf{0})} = \mathrm{Re}\Big[B_0(-\omega^2;M^2,M^2)\Big] \\
&\quad = \frac{1}{(4\pi)^2}\bigg[\frac{1}{\epsilon}+\ln\frac{\bar{\mu}^2}{M^2}+2-\frac{2(\omega^2-4M^2)^{\frac{1}{2}}}{\omega}\,\mathrm{acosh}\bigg(\frac{\omega}{2M}\bigg)+\mathcal{O}(\epsilon)\bigg]\,, \quad \omega>2M\,. \qquad \text{(B.43)}
\end{aligned}$$

Combining this with $S_1(\omega)$, and keeping the exponentially small terms in the coefficient of the divergence, we arrive at

$$\begin{aligned}
S_6^2(\omega) &= \theta(\omega-2M)\frac{(\omega^2-4M^2)^{\frac{1}{2}}}{2\omega(4\pi)^3}\tanh\Big(\frac{\beta\omega}{4}\Big)\times \qquad \text{(B.44)} \\
&\times \bigg[\frac{1}{\epsilon}+\ln\frac{\bar{\mu}^4}{M^2(\omega^2-4M^2)}+4-\frac{2(\omega^2-4M^2)^{\frac{1}{2}}}{\omega}\,\mathrm{acosh}\bigg(\frac{\omega}{2M}\bigg)+\mathcal{O}(\epsilon,e^{-\beta M})\bigg]\,.
\end{aligned}$$

B.13. $\hat{S}_6^2$

The sum-integral $\hat{S}_6^2$ is defined as

$$\hat{S}_6^2(\omega) \equiv \mathrm{Disc}\,\bigg[\sum\!\!\!\!\!\!\int_{K\{P\}} \frac{1}{K^2}\frac{K^2\,[\mathbf{p}^2-(\mathbf{p}\cdot\hat{\mathbf{k}})^2]}{\Delta(P)\Delta(P-Q)\Delta(P-K)\Delta(P-Q-K)}\bigg]_{Q=(-i\omega,\mathbf{0})}\,. \qquad \text{(B.45)}$$

The summation factorizes into two independent parts like for S_6^2; however, the spatial integrations do not factorize due to the additional structure in the numerator. Therefore the evaluation is somewhat more involved, yet the general techniques introduced in appendix A yield a solution:

$$\begin{aligned}
\hat{S}_6^2(\omega) &= \theta(\omega-2M)\frac{(\omega^2-4M^2)^{\frac{3}{2}}}{12\omega(4\pi)^3}\tanh\Big(\frac{\beta\omega}{4}\Big)\times \qquad \text{(B.46)} \\
&\times \bigg[\frac{1}{\epsilon}+\ln\frac{\bar{\mu}^4}{M^2(\omega^2-4M^2)}+4+\frac{\omega^2+2M^2}{3(\omega^2-4M^2)} \\
&\qquad -\frac{2(\omega^4-6\omega^2M^2+12M^4)}{\omega(\omega^2-4M^2)^{\frac{3}{2}}}\,\mathrm{acosh}\bigg(\frac{\omega}{2M}\bigg)+\mathcal{O}(\epsilon,e^{-\beta M})\bigg]\,.
\end{aligned}$$

B.14. S_6^4

The sum-integral S_6^4 is defined as

$$S_6^4(\omega) \equiv \mathrm{Disc}\left[\sum\!\!\!\!\!\!\int_{K\{P\}} \frac{1}{K^2}\frac{(K^2)^2}{\Delta(P)\Delta(P-Q)\Delta(P-K)\Delta(P-Q-K)}\right]_{Q=(-i\omega,\mathbf{0})} . \tag{B.47}$$

Like with S_4^2, S_5^2 and S_6^2, we proceed directly with free gluons rather than using the spectral representation. Cancelling one K^2 and carrying out the shift $K \to P-K$, we get

$$S_6^4(\omega) = \mathrm{Disc}\left[\sum\!\!\!\!\!\!\int_{\{K,P\}} \frac{\Delta(P)+\Delta(K)-2(M^2+P\cdot K)}{\Delta(P)\Delta(P-Q)\Delta(K)\Delta(K-Q)}\right]_{Q=(-i\omega,\mathbf{0})} . \tag{B.48}$$

Another change of integration variables, $P \to Q-P$, shows that

$$\sum\!\!\!\!\!\!\int_{\{P\}} \frac{P}{\Delta(P)\Delta(P-Q)} = \frac{Q}{2}\sum\!\!\!\!\!\!\int_{\{P\}} \frac{1}{\Delta(P)\Delta(P-Q)} , \tag{B.49}$$

and similarly for the term with $\sum\!\!\!\!\!\!\int_{\{K\}}$. Thereby we arrive at

$$\begin{aligned} S_6^4(\omega) &= 2S_4^2(\omega) + \frac{1}{2}(\omega^2-4M^2)S_6^2(\omega) && \text{(B.50)}\\ &= \theta(\omega-2M)\frac{(\omega^2-4M^2)^{\frac{1}{2}}}{4\omega(4\pi)^3}\tanh\Big(\frac{\beta\omega}{4}\Big)\times \\ &\times \Bigg\{(\omega^2-6M^2)\left[\frac{1}{\epsilon}+\ln\frac{\bar{\mu}^4}{M^2(\omega^2-4M^2)}+3\right] \\ &\quad +(\omega^2-4M^2)\left[1-\frac{2(\omega^2-4M^2)^{\frac{1}{2}}}{\omega}\,\mathrm{acosh}\left(\frac{\omega}{2M}\right)\right]+\mathcal{O}(\epsilon,e^{-\beta M})\Bigg\} . && \text{(B.51)} \end{aligned}$$

Appendix C. Spectral function in the scalar channel

For completeness, we have worked out the spectral function corresponding to the scalar channel with the same methods as described above for the vector channel. It seems, though, that the physical significance is not clear in the scalar case: no direct relation to an observable, in the sense of eq. (2.2), has been worked out, as far as we know, and the computation as such appears to possess a number of ambiguities. In particular, the scalar density requires renormalization, and the renormalization factor cannot be uniquely specified; moreover the resummation of the spectral function within a potential model near the threshold appears to lead to ambiguities [8]. Nevertheless, on the lattice the correlator of (bare) scalar densities can be treated on the same footing as that of the vector currents [21, 22].

Concerning the first of the issues, namely renormalization, the method we choose is to consider the object

$$\hat{\mathcal{S}} \equiv M_B^{(\delta)}\, \hat{\bar{\psi}}\, \hat{\psi}\;, \tag{C.1}$$

where $M_B^{(\delta)}$ is essentially the bare quark mass defined in eq. (3.7), only with a possible additional constant as a "probe",

$$\left(M_B^{(\delta)}\right)^2 \equiv M^2 - \frac{6g^2 C_F M^2}{(4\pi)^2}\left(\frac{1}{\epsilon} + \ln\frac{\bar{\mu}^2}{M^2} + \frac{4}{3} + \delta\right) + \mathcal{O}(g^4)\;. \tag{C.2}$$

We then define

$$\rho_S(\omega) \equiv \int_{-\infty}^{\infty} \mathrm{d}t\, e^{i\omega t} \int \mathrm{d}^{3-2\epsilon}\mathbf{x} \left\langle \frac{1}{2}\left[\hat{\mathcal{S}}(t,\mathbf{x}), \hat{\mathcal{S}}(0,\mathbf{0})\right]\right\rangle\;, \tag{C.3}$$

which turns out to be finite. Starting again at 1-loop level, and omitting Q-independent terms which are killed by the discontinuity in eq. (2.5), we get

$$= \; [Q-\text{indep.}] - 2C_A M^2 \sum\!\!\!\!\!\!\int_{\{P\}} \frac{Q^2+4M^2}{\Delta(P)\Delta(P-Q)}\;. \tag{C.4}$$

The counterterm graph yields

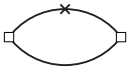

$$\begin{aligned} &= \; [Q-\text{indep.}] + \frac{12g^2 C_A C_F M^2}{(4\pi)^2}\left\{\left(\frac{1}{\epsilon} + \ln\frac{\bar{\mu}^2}{M^2} + \frac{4}{3}\right)\right. \\ &\times \; \left. \sum\!\!\!\!\!\!\int_{\{P\}} \left[\frac{Q^2+8M^2}{\Delta(P)\Delta(P-Q)} - \frac{2M^2(Q^2+4M^2)}{\Delta^2(P)\Delta(P-Q)}\right] + \delta \sum\!\!\!\!\!\!\int_{\{P\}} \frac{Q^2+4M^2}{\Delta(P)\Delta(P-Q)}\right\}. \end{aligned} \tag{C.5}$$

Finally, the genuine 2-loop graphs add up to

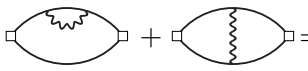

$$
\begin{aligned}
&= [Q-\text{indep.}] + 4g^2 C_A C_F M^2 \sum\!\!\!\!\!\!\int_{K\{P\}} \Bigg\{ \\
&\left(\frac{1}{K^2+\Pi_T} - \frac{1}{K^2+\Pi_E}\right)[\mathbf{p}^2 - (\mathbf{p}\cdot\hat{\mathbf{k}})^2] \times \\
&\qquad \times\left[-\frac{4(Q^2+4M^2)}{\Delta^2(P)\Delta(P-Q)\Delta(P-K)} - \frac{2(Q^2+4M^2)}{\Delta(P)\Delta(P-Q)\Delta(P-K)\Delta(P-Q-K)}\right] \\
&+ \frac{D-2}{K^2+\Pi_T}\left[\frac{Q^2+4M^2}{\Delta^2(P)\Delta(P-Q)} + \frac{2Q\cdot K}{\Delta(P)\Delta(P-Q)\Delta(P-K)}\right. \\
&\qquad \left. - \frac{(Q^2+4M^2)K^2}{\Delta^2(P)\Delta(P-Q)\Delta(P-K)} - \frac{\frac{1}{2}(Q^2+4M^2)K^2}{\Delta(P)\Delta(P-Q)\Delta(P-K)\Delta(P-Q-K)}\right] \\
&+ \frac{1}{K^2+\Pi_E}\left[-\frac{4(Q^2+4M^2)}{\Delta(P)\Delta(P-Q)\Delta(P-K)} + \frac{4(Q^2+4M^2)M^2}{\Delta^2(P)\Delta(P-Q)\Delta(P-K)}\right. \\
&\qquad \left. + \frac{(Q^2+2M^2)(Q^2+4M^2)+Q^2K^2}{\Delta(P)\Delta(P-Q)\Delta(P-K)\Delta(P-Q-K)}\right] \Bigg\} \,. \qquad \text{(C.6)}
\end{aligned}
$$

Again any dependence on the gauge parameter ξ has disappeared, and $P^E_{\mu\nu}$ of eq. (3.2) could have been replaced with $\delta_{\mu\nu} - P^T_{\mu\nu}$.

We note that the master sum-integrals appearing in eq. (C.6) are a subset of those in eq. (3.11). Therefore the discussion in sec. 3.4 continues to hold, and there are no infrared divergences in the result, so that we can set $\Pi_T = \Pi_E = 0$ in eq. (C.6). The full result can now be written as

$$
\begin{aligned}
\rho_S(\omega)\big|_{\rm raw} \;=\; & 2C_A M^2(\omega^2-4M^2)S_1(\omega) + 4g^2 C_A C_F M^2 \Bigg\{ \\
& \left[-\frac{3}{(4\pi)^2}\left(\frac{1}{\epsilon} + \ln\frac{\bar\mu^2}{M^2} + \frac{4}{3}\right)\right](\omega^2-8M^2)S_1(\omega) - \frac{3\delta}{(4\pi)^2}(\omega^2-4M^2)S_1(\omega) \\
& - \left[\frac{T^2}{6} - \frac{6M^2}{(4\pi)^2}\left(\frac{1}{\epsilon} + \ln\frac{\bar\mu^2}{M^2} + \frac{4}{3}\right)\right](\omega^2-4M^2)S_2(\omega) \\
& + 4(\omega^2-4M^2)S_4^0(\omega) + 4(1-\epsilon)S_4^1(\omega) - 2(\omega^2-4M^2)\Big[2M^2 S_5^0(\omega) - (1-\epsilon)S_5^2(\omega)\Big] \\
& + (\omega^2-2M^2)(\omega^2-4M^2)S_6^0(\omega) - \Big[\epsilon\omega^2 + 4(1-\epsilon)M^2\Big]S_6^2(\omega)\Bigg\} + \mathcal{O}(\epsilon) \,. \qquad \text{(C.7)}
\end{aligned}
$$

We have set here $\epsilon \to 0$ whenever the master sum-integral that it multiplies is finite.

Now, the structure of eq. (C.7) reveals an ambiguity with regard to the treatment of the "resummation" of thermal mass corrections, which in the vector case lead to eq. (4.3). In the vector case, the need to resum is unambiguous, because anything else than eq. (4.3) would lead to a thermal correction diverging at the threshold. In the scalar case, we do not have this guidance: terms multiplied by T^2 vanish as $\theta(\omega-2M)(\omega-2M)^{\frac{1}{2}}$ at the threshold,

being thus subdominant with respect to the leading thermal corrections which remain non-zero. Nevertheless, we would like to apply a "universal" thermal resummation, i.e. precisely eq. (4.3); however, it may be questioned whether it is valid to do this also in the term M^2, coming from the ("ultraviolet-completed") definition of the scalar current, or only in more infrared sensitive parts. It seems to us that this question can be fully settled only through a next-to-next-to-leading order computation; in the following, we assume that the resummation of eq. (4.3) is only carried out in the Lagrangian, not in the definition of the scalar density. If so, a redefinition of the mass according to eq. (4.3) leads to the modified result

$$\begin{aligned}
\rho_S(\omega) \,=\, & 2C_A M^2(\omega^2-4M^2)S_1(\omega) + 4g^2 C_A C_F M^2 \Bigg\{ \\
& \frac{T^2}{3} S_1(\omega) - \frac{3\delta}{(4\pi)^2}(\omega^2-4M^2)S_1(\omega) \\
& - \frac{3}{(4\pi)^2}\left(\frac{1}{\epsilon} + \ln\frac{\bar{\mu}^2}{M^2} + \frac{4}{3}\right)\Big[(\omega^2-8M^2)S_1(\omega) - 2M^2(\omega^2-4M^2)S_2(\omega)\Big] \\
& + 4(\omega^2-4M^2)S_4^0(\omega) + 4(1-\epsilon)S_4^1(\omega) - 2(\omega^2-4M^2)\Big[2M^2 S_5^0(\omega) - (1-\epsilon)S_5^2(\omega)\Big] \\
& + (\omega^2-2M^2)(\omega^2-4M^2)S_6^0(\omega) - \Big[\epsilon\omega^2 + 4(1-\epsilon)M^2\Big]S_6^2(\omega)\Bigg\} + \mathcal{O}(\epsilon) \,.
\end{aligned} \tag{C.8}$$

Unfortunately, the issue of what is resummed is not insignificant in the sense that the difference between eqs. (C.7) and (C.8) is numerically of $\mathcal{O}(1)$ for $\omega > 2M$.

Inserting the explicit expressions for the functions $S_i^j(\omega)$ from appendix B into eq. (C.8), the final result for the vacuum part reads

$$\begin{aligned}
\rho_S(\omega)|^{\rm vac} = {} & \theta(\omega-2M)\frac{C_A M^2(\omega^2-4M^2)^{\frac{3}{2}}}{8\pi\omega} + \theta(\omega-2M)\frac{4g^2 C_A C_F M^2}{(4\pi)^3\omega^2}\Bigg\{ \\
& (\omega^2-2M^2)(\omega^2-4M^2)L_2\left(\frac{\omega-\sqrt{\omega^2-4M^2}}{\omega+\sqrt{\omega^2-4M^2}}\right) + \left(\frac{3}{2}\,\omega^4 - 2\omega^2M^2 - 13M^4\right)\operatorname{acosh}\left(\frac{\omega}{2M}\right) \\
& - \omega(\omega^2-4M^2)^{\frac{1}{2}}\left[(\omega^2-4M^2)\left(\ln\frac{\omega(\omega^2-4M^2)}{M^3} + \frac{3}{4}\,\delta\right) - \frac{3}{8}\,(3\omega^2-14M^2)\right]\Bigg\} + \mathcal{O}(\epsilon, g^4) \,,
\end{aligned} \tag{C.9}$$

where the function L_2 is defined in eq. (4.6). Let us note that although similar to the vector channel spectral function in eq. (4.5) at first sight, eq. (C.9) has also some significant differences; in particular, logarithms of ω/M do *not* cancel at $\omega \gg M$ any more, but the asymptotic behaviour becomes

$$\rho_S(\omega)|^{\rm vac} \quad \overset{\omega\gg M}{\approx} \quad -\frac{3g^2 C_A C_F \omega^2 M^2}{(4\pi)^3}\left(\ln\frac{\omega^2}{M^2} + \delta - \frac{3}{2}\right) . \tag{C.10}$$

As the dependence on δ and δ's definition through eq. (C.2) show, the logarithm is in some sense related to the need to renormalize the scalar density and its correlators.

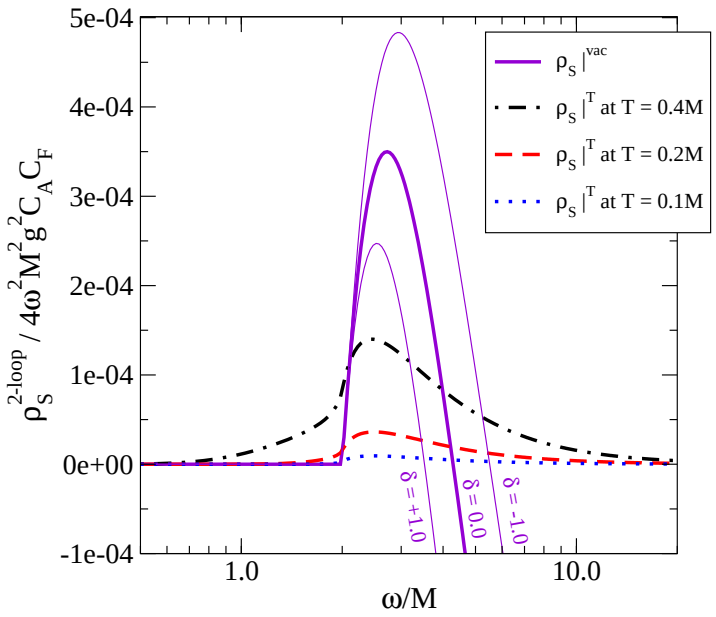

Figure 6: The vacuum and thermal parts of the next-to-leading order correction in the scalar channel, normalized by dividing with $4\omega^2 M^2 g^2 C_A C_F$. The vacuum part can become negative because the bare scalar correlator is multiplied with a bare mass parameter, cf. eqs. (C.1), (C.2); the constant δ illustrates how strong the dependence on the renormalization convention is.

The thermal correction, in turn, reads,

$$
\begin{aligned}
\rho_S(\omega)|^T \;=\; & \frac{4g^2 C_A C_F M^2}{(4\pi)^3\omega^2}\int_0^\infty \mathrm{d}k\,\frac{n_{\mathrm{B}}(k)}{k}\Big\{ \\
& \theta(\omega)\,\theta\Big(k-\frac{4M^2-\omega^2}{2\omega}\Big)\Big[-(\omega^2-4M^2)\sqrt{\omega(\omega+2k)}\sqrt{\omega(\omega+2k)-4M^2} \\
& \quad +2\Big((\omega^2-2M^2)(\omega^2-4M^2)+2\omega k(\omega^2-4M^2)+2\omega^2k^2\Big)\,\mathrm{acosh}\sqrt{\frac{\omega(\omega+2k)}{4M^2}}\Big] \\
+\;\; & \theta(\omega-2M)\,\theta\Big(\frac{\omega^2-4M^2}{2\omega}-k\Big)\Big[-(\omega^2-4M^2)\sqrt{\omega(\omega-2k)}\sqrt{\omega(\omega-2k)-4M^2} \\
& \quad +2\Big((\omega^2-2M^2)(\omega^2-4M^2)-2\omega k(\omega^2-4M^2)+2\omega^2k^2\Big)\,\mathrm{acosh}\sqrt{\frac{\omega(\omega-2k)}{4M^2}}\Big] \\
+\;\; & \theta(\omega-2M)\Big[2(\omega^2-4M^2+4k^2)\,\omega\sqrt{\omega^2-4M^2} \\
& \quad -4\Big((\omega^2-2M^2)(\omega^2-4M^2)+2\omega^2k^2\Big)\,\mathrm{acosh}\Big(\frac{\omega}{2M}\Big)\Big]\Big\}+\mathcal{O}(e^{-\beta M},g^4)\;,
\end{aligned}
\tag{C.11}
$$

where we represented T^2 as $\pi^2T^2 = 6\int_0^\infty \mathrm{d}k\,k\,n_{\mathrm{B}}(k)$.

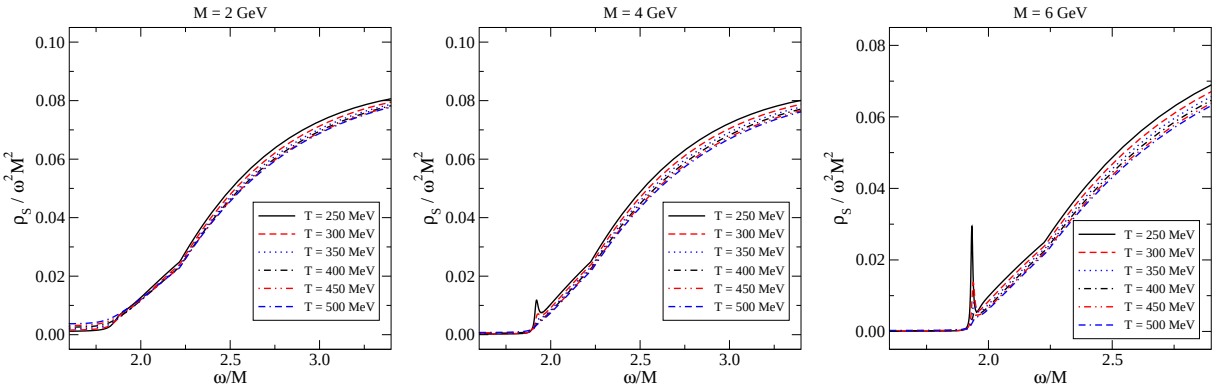

Figure 7: The phenomenologically assembled scalar channel spectral function $\rho_S(\omega)$, in units of $\omega^2 M^2$, for $M = 2, 4, 6$ GeV (from left to right). To the order considered, M is the heavy quark pole mass. Note that for better visibility, the axis ranges are different in the rightmost figure. As discussed after eq. (C.14), we are not confident that these plots have a definite physical significance; the figures are meant for illustration only.

A numerical evaluation of this result, compared with the vacuum part of eq. (C.9), is shown in fig. 6. For small ω the thermal part appears to be somewhat more significant than in the case of the vector channel; this is because there is a cancellation of positive and negative contributions in the vacuum part, before the negative terms take over at large ω (cf. eq. (C.10)). The thermal part, in contrast, stays positive and vanishes rapidly at large ω.

We wish to draw attention to the amusing feature, already mentioned at the end of sec. 4, that while the next-to-leading order vacuum part is continuous, the next-to-leading order thermal part appears even to have a continuous first derivative. In the vector channel, in contrast, the next-to-leading order vacuum part is discontinuous at the threshold, while the next-to-leading order thermal part appears to be continuous (cf. fig. 1). In other words, the thermal part seems always to be one degree smoother than the vacuum part.

In order to now combine our result with that obtained within a resummed framework in ref. [8], we need to match the normalizations, in analogy with eq. (5.4). Indeed, employing the notation of eq. (5.1), the leading order vacuum result in eq. (C.9) becomes

$$\left.\frac{\rho_S(\omega)}{\omega^2 M^2}\right|_{\rm LO} = \theta(\omega - 2M)\frac{C_A v^3}{8\pi} \,, \tag{C.12}$$

while the next-to-leading order result can be expanded as

$$\left.\frac{\rho_S(\omega)}{\omega^2 M^2}\right|_{\rm NLO} = 4g^2 C_A C_F \theta(\omega - 2M)\left[\frac{v^2}{256\pi} - \frac{v^3}{128\pi^3}\left(1 + \frac{3}{2}\,\delta\right) + \mathcal{O}(v^4)\right] . \tag{C.13}$$

Since radiative corrections within a non-relativistic potential model always involve a power of v, it is possible to account for the second term in eq. (C.13), equalling $-g^2 C_F(1 + 3\delta/2)/4\pi^2$

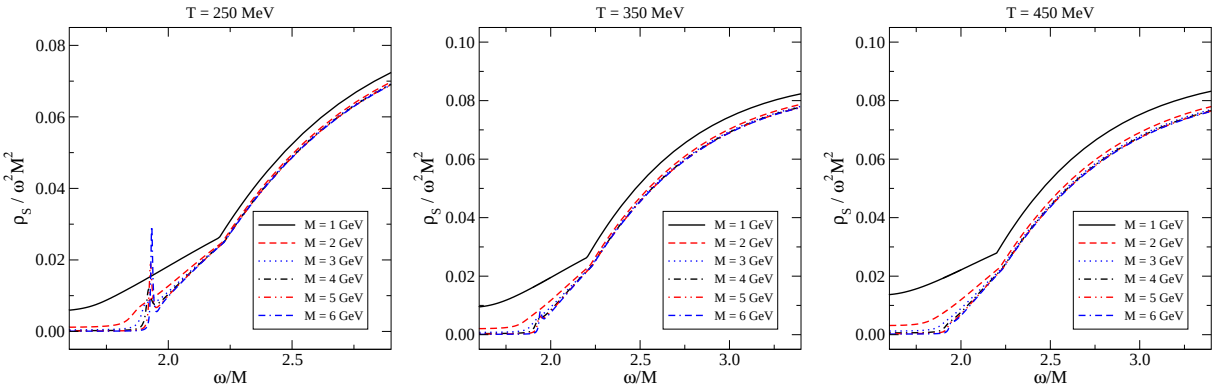

Figure 8: The phenomenologically assembled scalar channel spectral function $\rho_S(\omega)$, in units of $\omega^2 M^2$, for $T = 250, 350, 450$ MeV (from left to right). To the order considered, M is the heavy quark pole mass. Note that for better visibility, the axis ranges are different in the leftmost figure. As discussed after eq. (C.14), we are not confident that these plots have a definite physical significance; the figures are meant for illustration only.

times the leading term in eq. (5.2), only by a multiplicative correction of the scalar density,

$$\mathcal{S}_{\rm QCD} = \mathcal{S}_{\rm NRQCD}\left[1 - \frac{g^2 C_F}{8\pi^2}\left(1 + \frac{3}{2}\,\delta\right) + ...\right] . \tag{C.14}$$

Even though closer to unity than in eq. (5.4), the normalization factor could be numerically significant. In fact, if we leave the normalization factor open, and search for a value minimizing the squared difference of the resummed and QCD results (with $\delta = 0$) in the range $(\omega - 2M)/M = 0.0 - 0.4$ (thereby also accounting for thermal corrections), we find a best fit with an overall normalization factor $0.4 - 0.6$, i.e. with a *larger reduction* than in the vector case, in contrast to what eq. (C.14) would suggest.[5] This is perhaps another indication that the treatment of $\rho_S(\omega)$ within a Schrödinger-equation based resummed framework as in ref. [8] may not capture the correct physics.

Nevertheless, putting this worry aside for a moment, we again construct an "assembled" result as $\rho_S^{\rm (assembled)} \equiv \max(\rho_S^{\rm (QCD)}, \rho_S^{\rm (resummed)})$. The numerical value of the gauge coupling is taken from eq. (5.5). The outcome is shown in figs. 7, 8 for $\delta = 0$ and for various masses and temperatures, as a function of ω. Compared with the results in ref. [8], the overall magnitude is smaller by about $40 - 60\%$. At the same time, as is obvious from the plots, the two results do not interpolate to each other well; we have no explanation for this at the moment, but wish to repeat our concerns on the validity of the resummed near-threshold function $\rho_S^{\rm (resummed)}$.

[5]We note, however, that if we introduce another fit parameter, a horizontal energy shift, then the two results can be matched smoothly, with a multiplicative factor close to unity. We have not used this method in the plots because we prefer a universal procedure for the scalar and vector cases.

References

[1] G. Källén and A. Sabry, Kong. Dan. Vid. Sel. Mat. Fys. Med. 29N17 (1955) 1; J.S. Schwinger, *Particles, Sources and Fields. Volume II*, p. 407 (Addison-Wesley, 1973).

[2] R. Barbieri and E. Remiddi, Nuovo Cim. A 13 (1973) 99.

[3] D.J. Broadhurst, J. Fleischer and O.V. Tarasov, Z. Phys. C 60 (1993) 287 [hep-ph/9304303].

[4] A.H. Hoang, V. Mateu and S. Mohammad Zebarjad, 0807.4173.

[5] L.D. McLerran and T. Toimela, Phys. Rev. D 31 (1985) 545; H.A. Weldon, Phys. Rev. D 42 (1990) 2384; C. Gale and J.I. Kapusta, Nucl. Phys. B 357 (1991) 65.

[6] T. Matsui and H. Satz, Phys. Lett. B 178 (1986) 416.

[7] M. Laine, O. Philipsen, P. Romatschke and M. Tassler, JHEP 03 (2007) 054 [hep-ph/0611300]; M. Laine, JHEP 05 (2007) 028 [0704.1720]; M. Laine, O. Philipsen and M. Tassler, JHEP 09 (2007) 066 [0707.2458].

[8] Y. Burnier, M. Laine and M. Vepsäläinen, JHEP 01 (2008) 043 [0711.1743].

[9] A. Beraudo, J.P. Blaizot and C. Ratti, Nucl. Phys. A 806 (2008) 312 [0712.4394].

[10] M.A. Escobedo and J. Soto, 0804.0691.

[11] N. Brambilla, J. Ghiglieri, A. Vairo and P. Petreczky, Phys. Rev. D 78 (2008) 014017 [0804.0993].

[12] M. Laine, 0810.1112.

[13] F. Dominguez and B. Wu, 0811.1058.

[14] R. Rapp, D. Blaschke and P. Crochet, 0807.2470.

[15] A. Mócsy, 0811.0337.

[16] O. Philipsen, 0810.4685.

[17] R.C. Myers, A.O. Starinets and R.M. Thomson, JHEP 11 (2007) 091 [0706.0162].

[18] A.D. Linde, Phys. Lett. B 96 (1980) 289; D.J. Gross, R.D. Pisarski and L.G. Yaffe, Rev. Mod. Phys. 53 (1981) 43.

[19] F. Di Renzo, M. Laine, V. Miccio, Y. Schröder and C. Torrero, JHEP 07 (2006) 026 [hep-ph/0605042].

[20] G. Cuniberti, E. De Micheli and G.A. Viano, Commun. Math. Phys. 216 (2001) 59 [cond-mat/0109175].

[21] A. Jakovác, P. Petreczky, K. Petrov and A. Velytsky, Phys. Rev. D 75 (2007) 014506 [hep-lat/0611017]; G. Aarts, C. Allton, M.B. Oktay, M. Peardon and J.I. Skullerud, Phys. Rev. D 76 (2007) 094513 [0705.2198].

[22] P. Petreczky, 0810.0258.

[23] F. Karsch, E. Laermann, P. Petreczky and S. Stickan, Phys. Rev. D 68 (2003) 014504 [hep-lat/0303017]; G. Aarts and J.M. Martínez Resco, Nucl. Phys. B 726 (2005) 93 [hep-lat/0507004]; A. Mócsy and P. Petreczky, Phys. Rev. D 73 (2006) 074007 [hep-ph/0512156]; G. Aarts and J. Foley, JHEP 02 (2007) 062 [hep-lat/0612007].

[24] R.V. Harlander and M. Steinhauser, Comput. Phys. Commun. 153 (2003) 244 [hep-ph/0212294].

[25] M. Le Bellac, *Thermal Field Theory* (Cambridge University Press, Cambridge, 2000).

[26] J.I. Kapusta and C. Gale, *Finite-Temperature Field Theory: Principles and Applications* (Cambridge University Press, Cambridge, 2006).

[27] V.P. Silin, Sov. Phys. JETP 11 (1960) 1136 [Zh. Eksp. Teor. Fiz. 38 (1960) 1577]; V.V. Klimov, Sov. Phys. JETP 55 (1982) 199 [Zh. Eksp. Teor. Fiz. 82 (1982) 336]; H.A. Weldon, Phys. Rev. D 26 (1982) 1394.

[28] R.D. Pisarski, Phys. Rev. Lett. 63 (1989) 1129; J. Frenkel and J.C. Taylor, Nucl. Phys. B 334 (1990) 199; E. Braaten and R.D. Pisarski, Nucl. Phys. B 337 (1990) 569; J.C. Taylor and S.M.H. Wong, Nucl. Phys. B 346 (1990) 115.

[29] J.F. Donoghue, B.R. Holstein and R.W. Robinett, Annals Phys. 164 (1985) 233 [Erratum-ibid. 172 (1986) 483].

[30] W.E. Caswell and G.P. Lepage, Phys. Lett. B 167 (1986) 437.

[31] J.G. Körner and G. Thompson, Phys. Lett. B 264 (1991) 185.

[32] A. Pineda and J. Soto, Nucl. Phys. B (Proc. Suppl.) 64 (1998) 428 [hep-ph/9707481].

[33] N. Brambilla, A. Pineda, J. Soto and A. Vairo, Nucl. Phys. B 566 (2000) 275 [hep-ph/9907240].

[34] M. Beneke, Y. Kiyo and A.A. Penin, Phys. Lett. B 653 (2007) 53 [0706.2733].

[35] A. Czarnecki and K. Melnikov, Phys. Rev. Lett. 80 (1998) 2531 [hep-ph/9712222]; M. Beneke, A. Signer and V.A. Smirnov, Phys. Rev. Lett. 80 (1998) 2535 [hep-ph/9712302].

[36] M. Laine and Y. Schröder, JHEP 03 (2005) 067 [hep-ph/0503061].

[37] K. Kajantie, M. Laine, K. Rummukainen and M. Shaposhnikov, Nucl. Phys. B 503 (1997) 357 [hep-ph/9704416].

[38] E. Braaten and M.H. Thoma, Phys. Rev. D 44 (1991) 2625; G.D. Moore and D. Teaney, Phys. Rev. C 71 (2005) 064904 [hep-ph/0412346]; P. Petreczky and D. Teaney, Phys. Rev. D 73 (2006) 014508 [hep-ph/0507318].

[39] S. Caron-Huot and G.D. Moore, JHEP 02 (2008) 081 [0801.2173].